

Signals for New Physics in Rare Decays

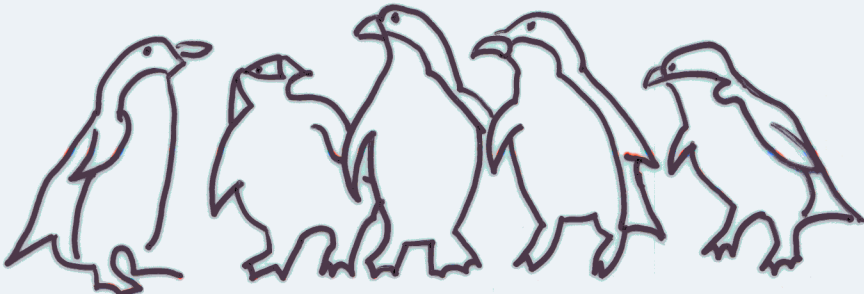
Overview... For details see:

M. Misiak : SM $B \rightarrow X_s \gamma$ Computations

G. Burdman: Exclusive $B \rightarrow K/K^* l\bar{l}$

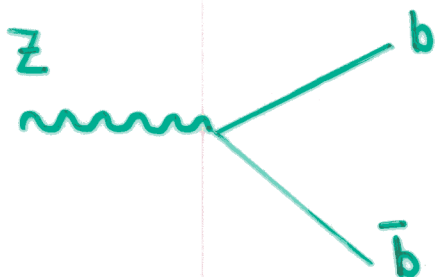
G. Hiller : Inclusive $B \rightarrow X_s l^+l^-$

J. Hewett
SLAC '02

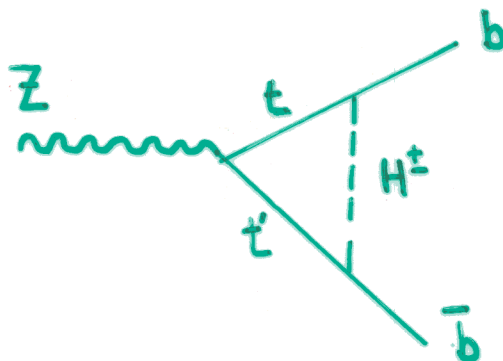


FCNC have longstanding history of
providing strong model building constraints

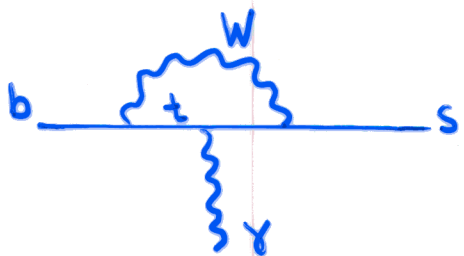
Precision EW:



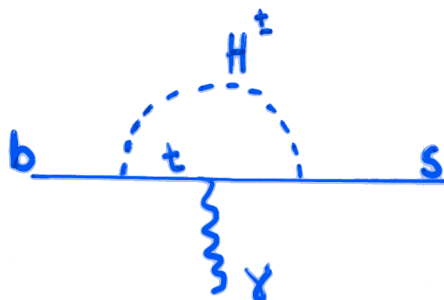
vs.



Rare Decays:



vs.



$B \rightarrow X_s \gamma$ Constrains Supersymmetry!

Constrained
mSSM

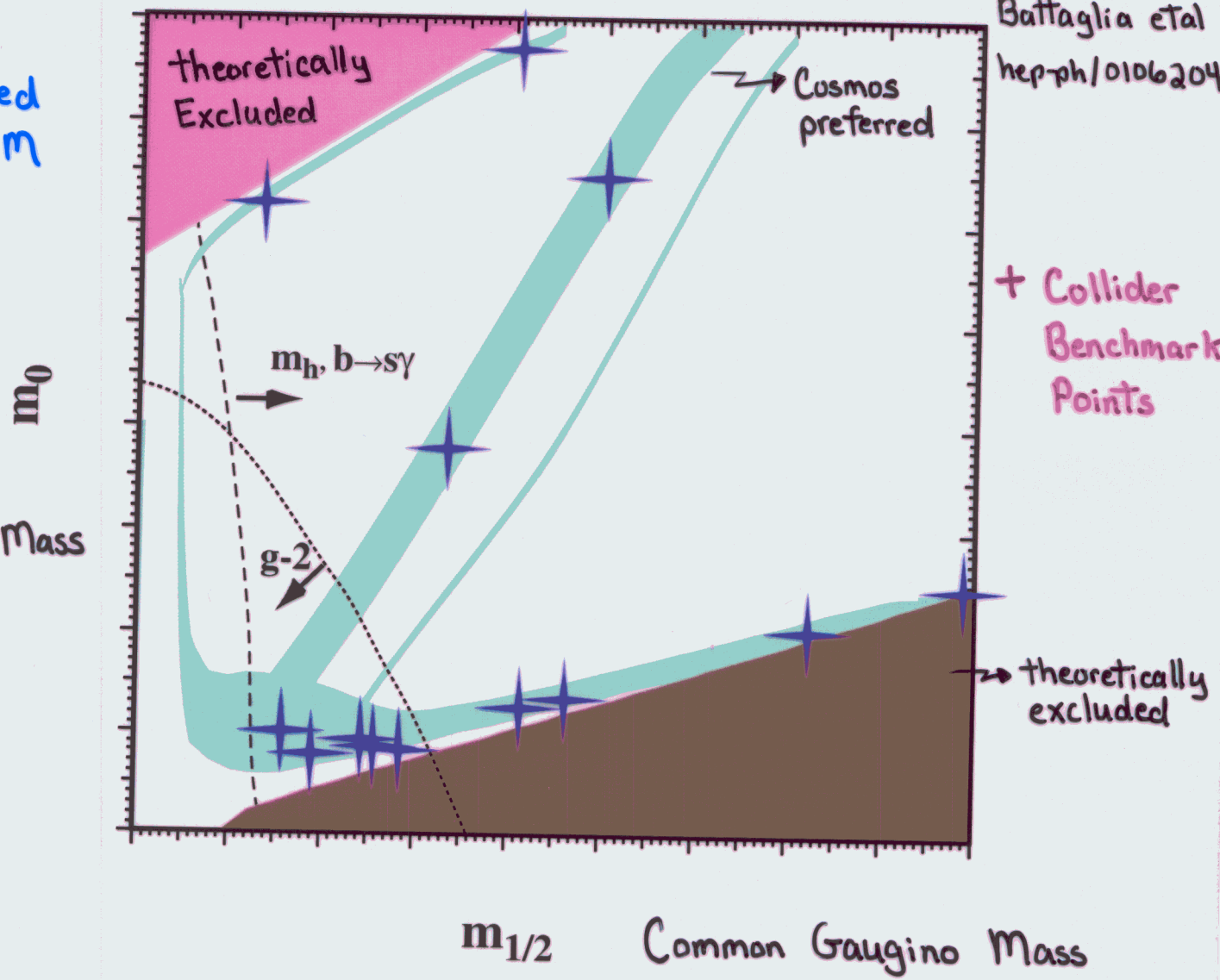
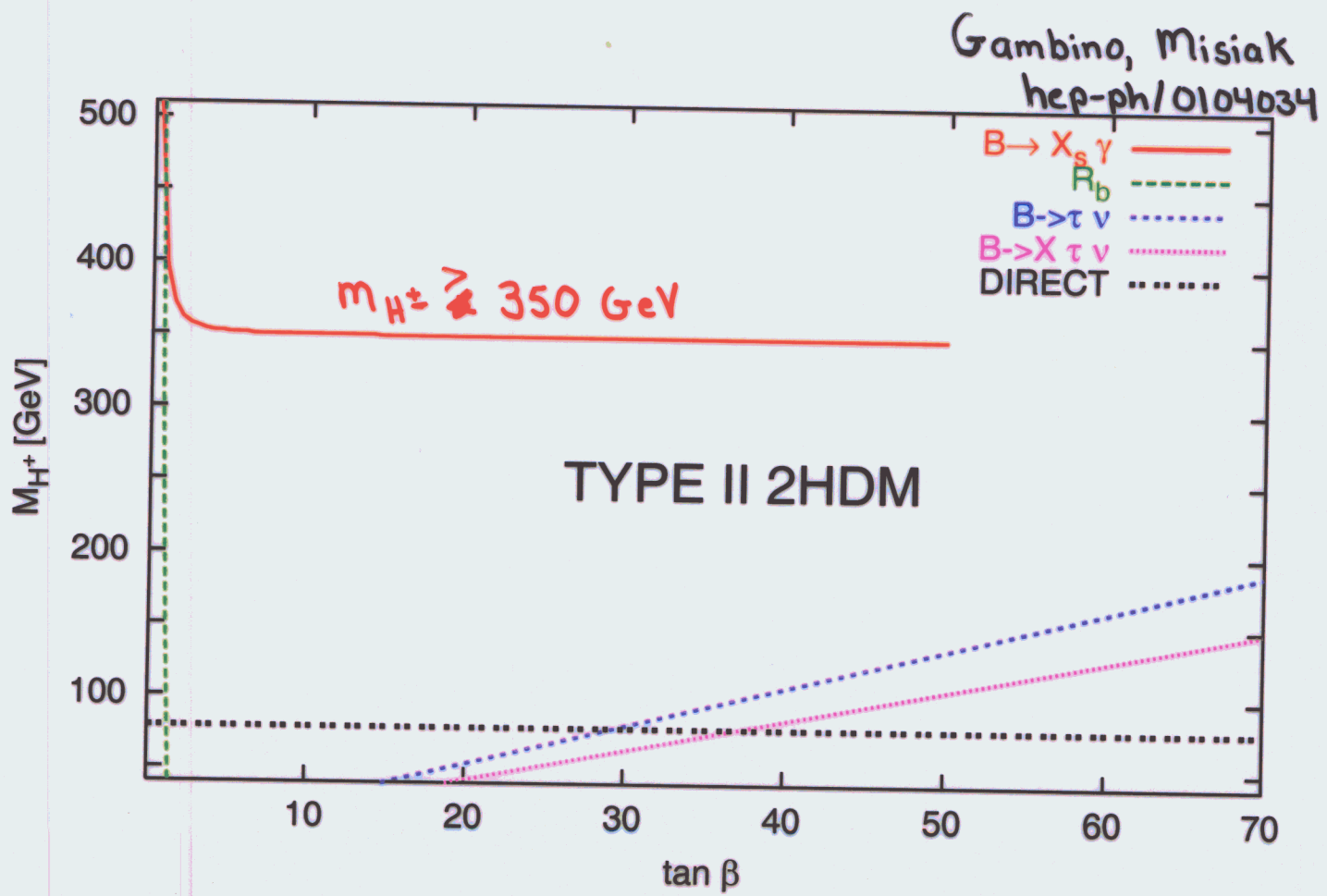


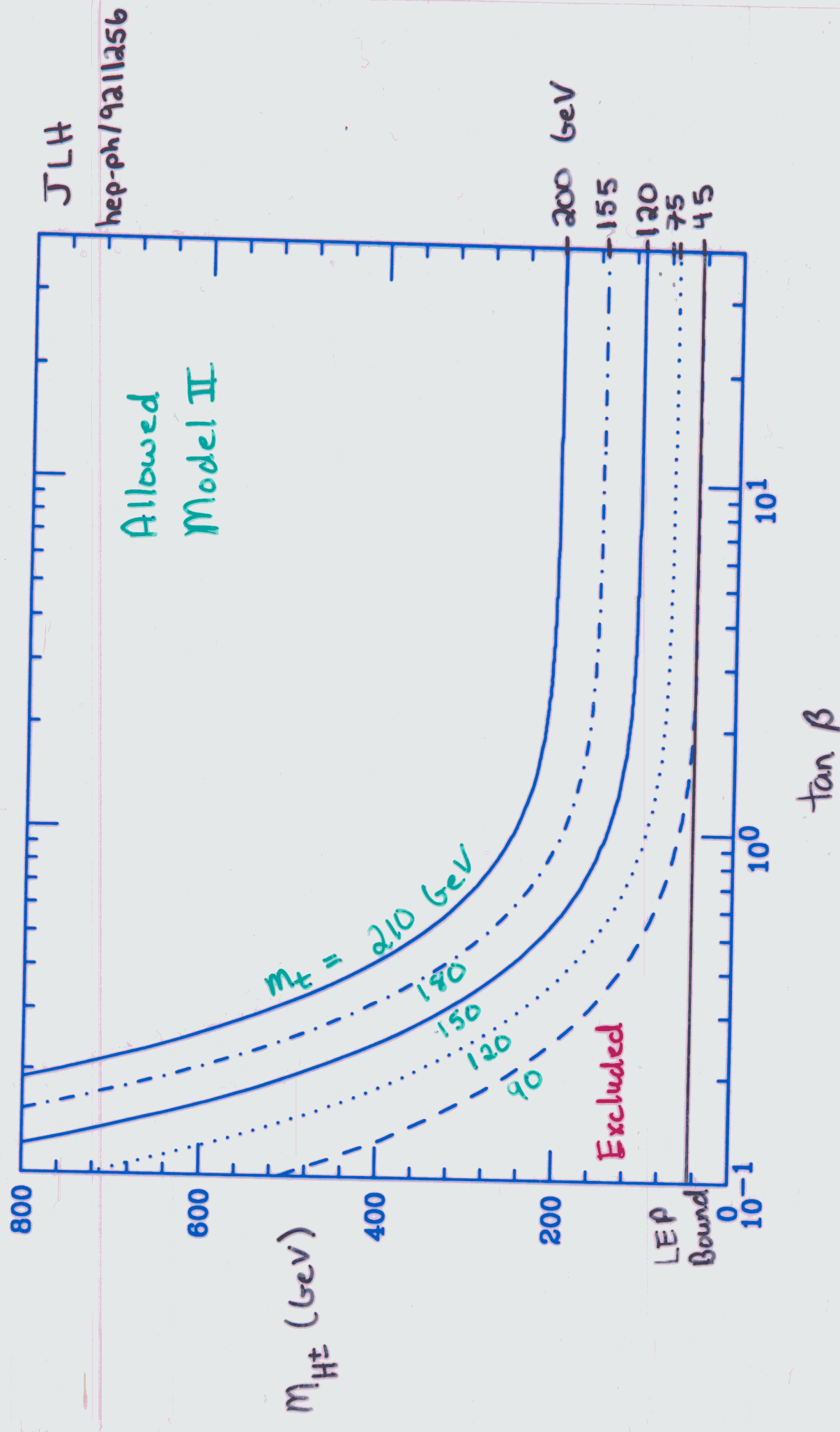
Figure 1: Qualitative overview of the locations of our proposed benchmark points in a generic $(m_{1/2}, m_0)$ plane. The light (turquoise) shaded area is the cosmologically preferred region with $0.1 \leq \Omega_\chi h^2 \leq 0.3$, whose exact shape depends on the value of $\tan \beta$, and to some extent on the Standard Model inputs m_t , m_b and α_s . In the dark (brick red) shaded region at bottom right, the LSP is the charged $\tilde{\tau}_1$, so this region is excluded. Electroweak symmetry breaking is not possible in the dark (pink) shaded region at top left. The LEP experimental constraints, in particular that on m_h , and measurements of $b \rightarrow s\gamma$ exert pressure from the left side. The BNL E821 measurement of $g_\mu - 2$ favours relatively low values of m_0 and $m_{1/2}$ for $\mu > 0$. The CMSSM benchmark points we propose are indicated roughly by the (blue) crosses. We propose points in the ‘bulk’ region at bottom left, along the coannihilation ‘tail’ extending to larger $m_{1/2}$, in the ‘focus-point’ region at large m_0 , and in the rapid-annihilation ‘funnel’ that may appear at intermediate $m_0/m_{1/2}$ for large $\tan \beta$.

Constraints on Two-Higgs Doublet Models



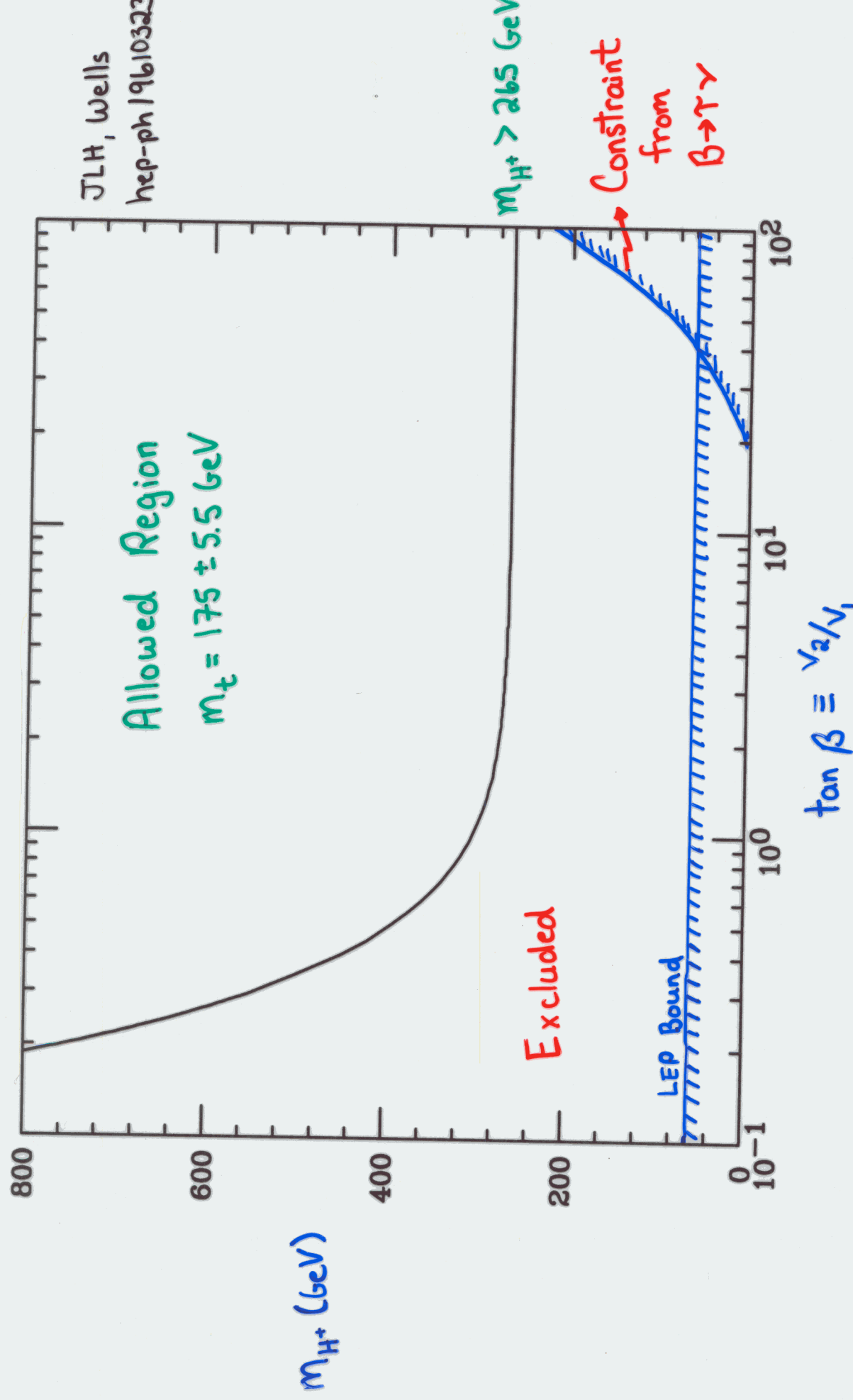
Circa '01

$$\mathcal{B}(b \rightarrow s\gamma) < 8.4 \times 10^{-4}$$



H^\pm bounds circa 1992 : Naive LO calculation

H^+ Constraints from $B \rightarrow X_s \chi$ - New 95% C.L. CLEO Bounds



Cira '96
Partial NLO

Surpasses Collider Reach!

Strong Interplay

Between

Theory and Experiment!

New Physics Searches require:

Precision Theory

+

Precision Experiment

Standard Model Computations

$B \rightarrow X_s \gamma$: NLO

$B \rightarrow X_s l^+ l^-$: NNLL



HUGE Effort from large theoretical
community!

QCD Corrections - Via Operator Mixing

Gilman + Wise

Operator Product Expansion

$$\mathcal{H}_{\text{eff}} = \frac{-4G_F}{\sqrt{2}} V_{q\bar{q}Q} V_{q'\bar{q}'Q}^* \sum_{i=1}^n C_i(\mu) O_i(\mu)$$

short distance,
perturbative
physics

non-pert.
physics

Calculate C_i at $\mu = m_w \Rightarrow$ matching conditions

Use RGE to evolve to $\mu \rightarrow m_b \rightarrow m_c \rightarrow m_k$

$$\mu \frac{d}{d\mu} \mathcal{H} = 0 \Rightarrow \mu \frac{d}{d\mu} C_i(\mu) = \gamma_{ij}^T(q_s) C_j(\mu)$$

anomalous dimension
matrix

Complete set of operators governing $\Delta Q=1$ transitions

$$\begin{aligned}
 O_1 &= (\bar{q}_b^\alpha \gamma_\mu P_L q_b^\beta)(\bar{q}_b^\beta \gamma^\mu P_L Q_\alpha) & O_2 &= (\bar{q}_b^\alpha \gamma_\mu P_L q_b^\beta)(\bar{q}_b^\beta \gamma^\mu P_L Q_\beta) \\
 O_3 &= (\bar{q}_b^\alpha \gamma_\mu P_L Q_\alpha) \sum_{q'} (\bar{q}_b^\beta \gamma^\mu P_L q_b'^\alpha) & O_4 &= (\bar{q}_b^\alpha \gamma_\mu P_L Q_\beta) \sum_{q'} (\bar{q}_b^\beta \gamma^\mu P_L q_b'^\alpha) \\
 O_5 &= (\bar{q}_b^\alpha \gamma_\mu P_L Q_\alpha) \sum_{q'} (\bar{q}_b^\beta \gamma^\mu P_R q_b'^\beta) & O_6 &= (\bar{q}_b^\alpha \gamma_\mu P_L Q_\beta) \sum_{q'} (\bar{q}_b^\beta \gamma^\mu P_R q_b'^\alpha) \\
 O_7 &= \frac{e}{16\pi^2} m_Q (\bar{q}_b^\alpha \sigma_{\mu\nu} P_R Q_\alpha) F^{\mu\nu} & O_8 &= \frac{g_s}{16\pi^2} m_Q (\bar{q}_b^\alpha \sigma_{\mu\nu} T_{ab}^a P_R Q_\beta) G^{a\mu\nu} \\
 O_9 &= \frac{e^2}{16\pi^2} (\bar{q}_b^\alpha \gamma_\mu P_L Q_\alpha) (\bar{l} \gamma^\mu l) & O_{10} &= \frac{e^2}{16\pi^2} (\bar{q}_b^\alpha \gamma_\mu P_L Q_\alpha) (\bar{l} \gamma^\mu \gamma_5 l)
 \end{aligned}$$

$B \rightarrow X_s \gamma$ at LO + NLO:

Wilson Coeff: NLO Matching Conditions

Buras et al
Lin, Liu, Yao
Greub, Hurth

LO Anomalous Dimension Matrix

Ciuchini et al
Cella et al
Misiak

NLO Anomalous Dimension Matrix Chetyrkin, Misiak, Müller

Matrix Element: NLO Virtual Corrections

Greub, Hurth, Wyler
Buras et al

Bremsstrahlung Corrections

Ali, Greub
Pott

Electroweak: 2-loop resummation

Czarnecki, Marciano
Baranowski, Misiak

E_γ Spectrum: Bremsstrahlung Corrections

Ali, Greub

Scale Dependence

Neubert, Kagan

Resummation of Threshold Logs Leibovich, Rothstein

SM Predictions:

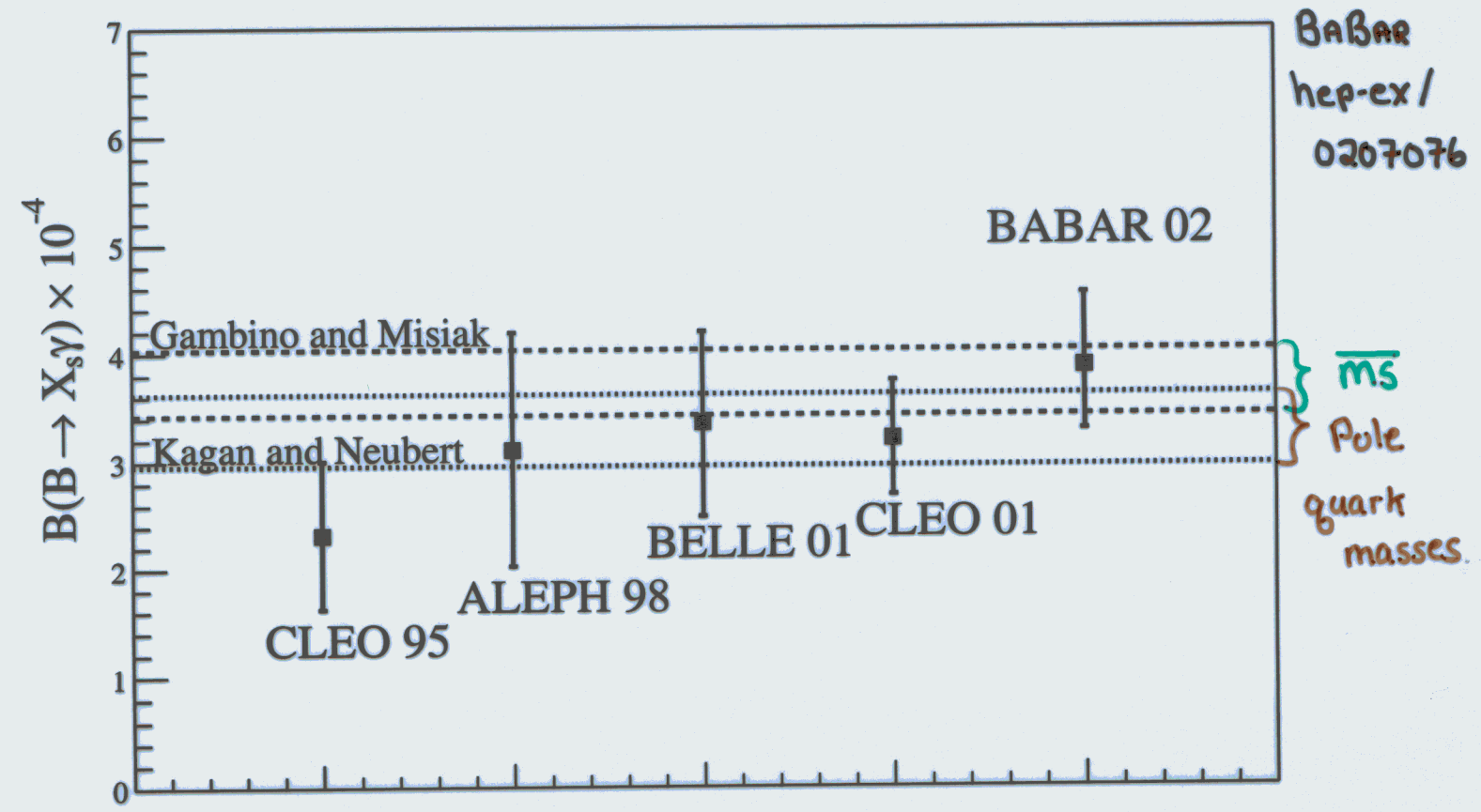
$$B(B \rightarrow X_s \gamma) = \begin{cases} (3.35 \pm 0.30) \times 10^{-4} & \text{pole quark masses} \\ (3.73 \pm 0.30) \times 10^{-4} & \overline{\text{MS}} \text{ quark masses} \end{cases}$$

Gambino, Misiak

Present theoretical error larger than usually assumed

A Tour de Force Effort!!

Comparison with Experiment



More

3-loop calculations have begun

See Misiak

CKM Fits

hep-ph/0206242

Ali ICHEP'02

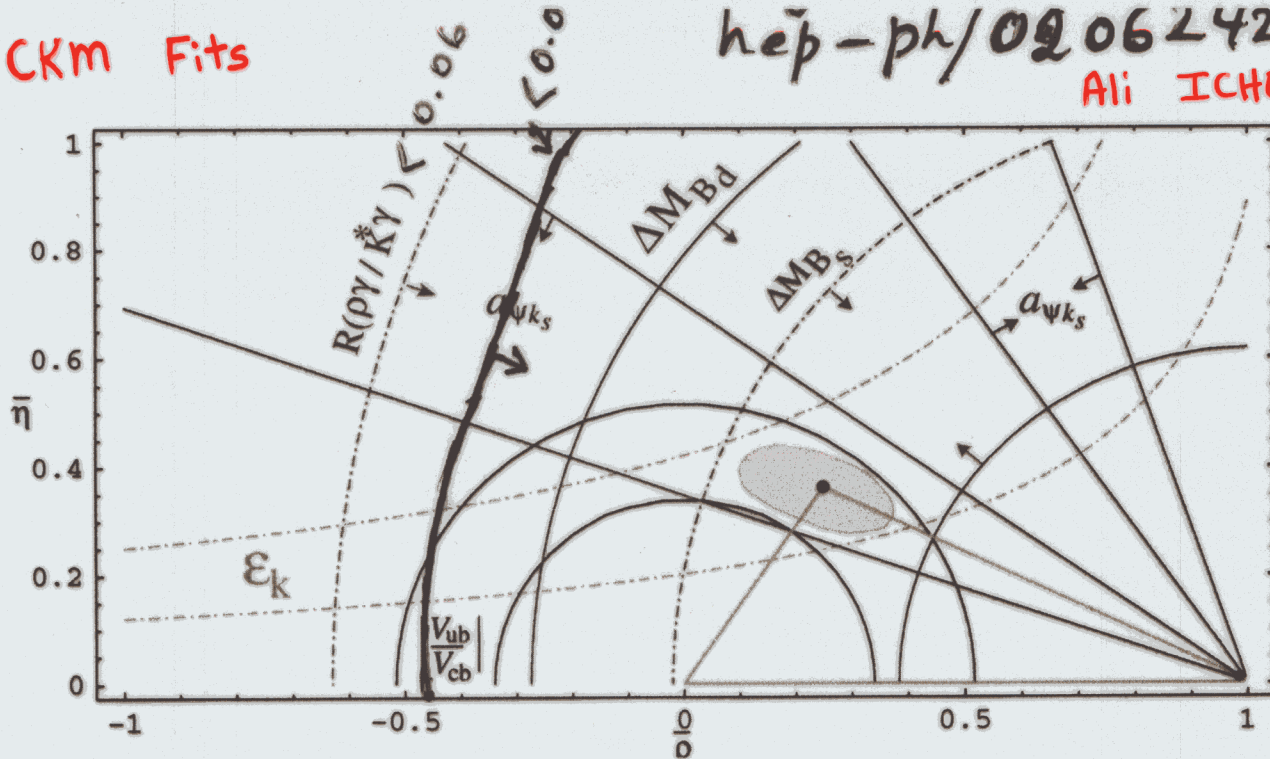


Figure 1: Unitary triangle fit in the SM and the resulting 95% C.L. contour in the $\bar{\rho}$ - $\bar{\eta}$ plane. The impact of the $R(\rho\gamma/K^*\gamma) < 0.06$ constraint is also shown.

Theoretical Uncertainties

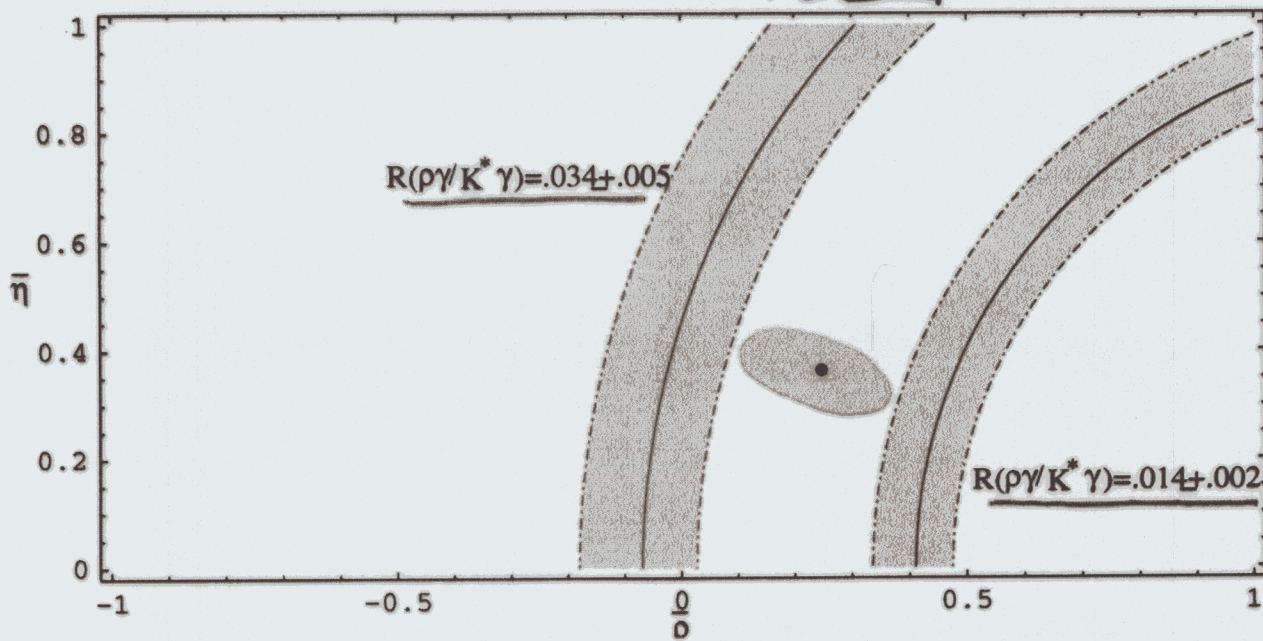
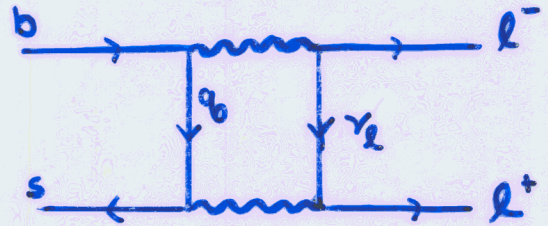
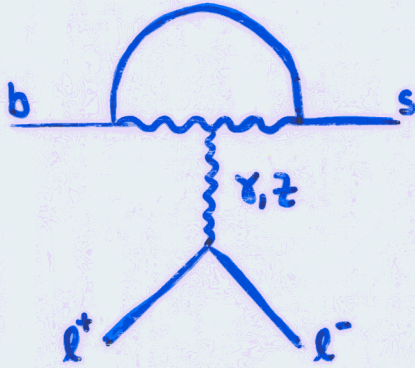
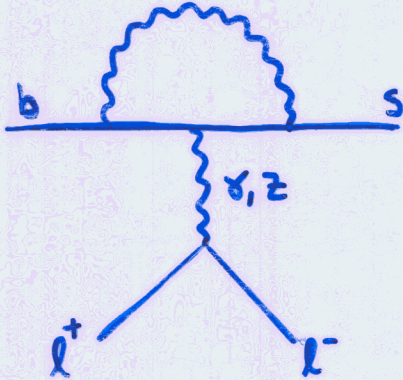


Figure 2: Extremal values of $R(\rho\gamma/K^*\gamma)$ that are compatible with the SM unitarity triangle analysis.

Need to reduce theoretical uncertainty
@ present $\delta(V_{td}) \approx 0(15\%)$

$B \rightarrow X_s \ell^+ \ell^-$



Computed to NLO

$$\mathcal{M} = \frac{\sqrt{2} G_F \alpha}{\pi} V_{tb} V_{ts}^* \left[C_q^{\text{eff}} \bar{s}_L \gamma_\mu b_L \bar{\ell} \gamma^\mu \ell + C_{10} \bar{s}_L \gamma_\mu b_L \bar{\ell} \gamma^\mu \gamma_5 \ell \right] - 2 C_7 m_b \bar{s}_L i \sigma_{\mu\nu} \frac{q^\nu}{q_b^2} b_R \bar{\ell} \gamma^\mu \ell$$

q_b^2 = momentum transfer to $\ell^+ \ell^-$ $(\hat{s} = q^2/m_b^2)$

Long distance resonance contributions

$B \rightarrow K^{(*)} \chi^{(0)} \rightarrow \ell^+ \ell^-$

peaks at $q_b^2 = m_{K^{(*)}}^2$

\Rightarrow Effective $(\bar{s}_L \gamma_\mu b_L)(\bar{\ell} \gamma^\mu \ell)$ interaction

$$C_q^{\text{eff}}(\mu) = C_q(\mu) + Y(\mu, \hat{s}) - \frac{3\pi}{\alpha^2 m_b^2} \sum_{K, K'} \frac{m_{V_i} \Gamma(V_i \rightarrow \ell^+ \ell^-)}{(\hat{s} - \frac{m_{V_i}^2}{m_b^2}) + i \frac{\Gamma_{V_i}}{m_b^2} m_{V_i}}$$

contribution from
c + light-quarks

Kinematic Distributions - Requires high statistics!

(Lim, Morozumi, Sanda)
 Deshpande et al
 Ali et al)

- $m_{l^+l^-}$ Distribution

$$\frac{d\Gamma(B \rightarrow X_S l^+ l^-)}{d\hat{s}} \sim (1-\hat{s})^2 \left[(|C_9^{\text{eff}}|^2 + |C_{10}|^2)(1+2\hat{s}) + 4|C_7|^2 \frac{2+\hat{s}}{\hat{s}} + 12 \operatorname{Re}(C_9^{\text{eff}} C_7) \right]$$

- Forward-Backward Asymmetry of l^+l^- angular distribution

$$A_{FB} = \frac{\int_0^1 dz \frac{d\Gamma}{dz d\hat{s}} - \int_{-1}^0 dz \frac{d\Gamma}{dz d\hat{s}}}{\int_0^1 dz \frac{d\Gamma}{dz d\hat{s}} + \int_{-1}^0 dz \frac{d\Gamma}{dz d\hat{s}}} \quad (\text{Ali et al})$$

$$= -3 C_{10} [\operatorname{Re} C_9^{\text{eff}} \hat{s} + 2 C_7] / d\Gamma/d\hat{s}$$

- Tau Polarization Asymmetry in $B \rightarrow X_S \tau^+ \tau^-$

$$P_\tau = \frac{d\Gamma_{\lambda=-1} - d\Gamma_{\lambda=+1}}{d\Gamma_{\lambda=-1} + d\Gamma_{\lambda=+1}} \quad (\text{JLH Kruger, Sehgal})$$

$$= -2 C_{10} [\operatorname{Re} C_9^{\text{eff}} F_1(\hat{s}, m_\tau) + 3 C_7 F_2(\hat{s}, m_\tau)] / d\Gamma_\tau/d\hat{s}$$

$B \rightarrow X_s l^+ l^-$ at NLO + NNLL

LO Estimate of $d\Gamma/d\hat{s}$

Grinstein, Savage, Wise '89

Matching Conditions: NLL

Misiak
Buras, Munz

NNLO

Bobeth, Misiak, Urban

Matrix Elements: 2-loop virtual corrections

Asatrian, Greub, Walker
Asatryan

Bremsstrahlung corrections

Asatryan, Asatrian,
Greub, Walker

Leading Power Corrections: $1/m_b$

Falk, Luke, Savage
Ali, Hiller, Handoko, Morozumi
Buchalla, Isidori

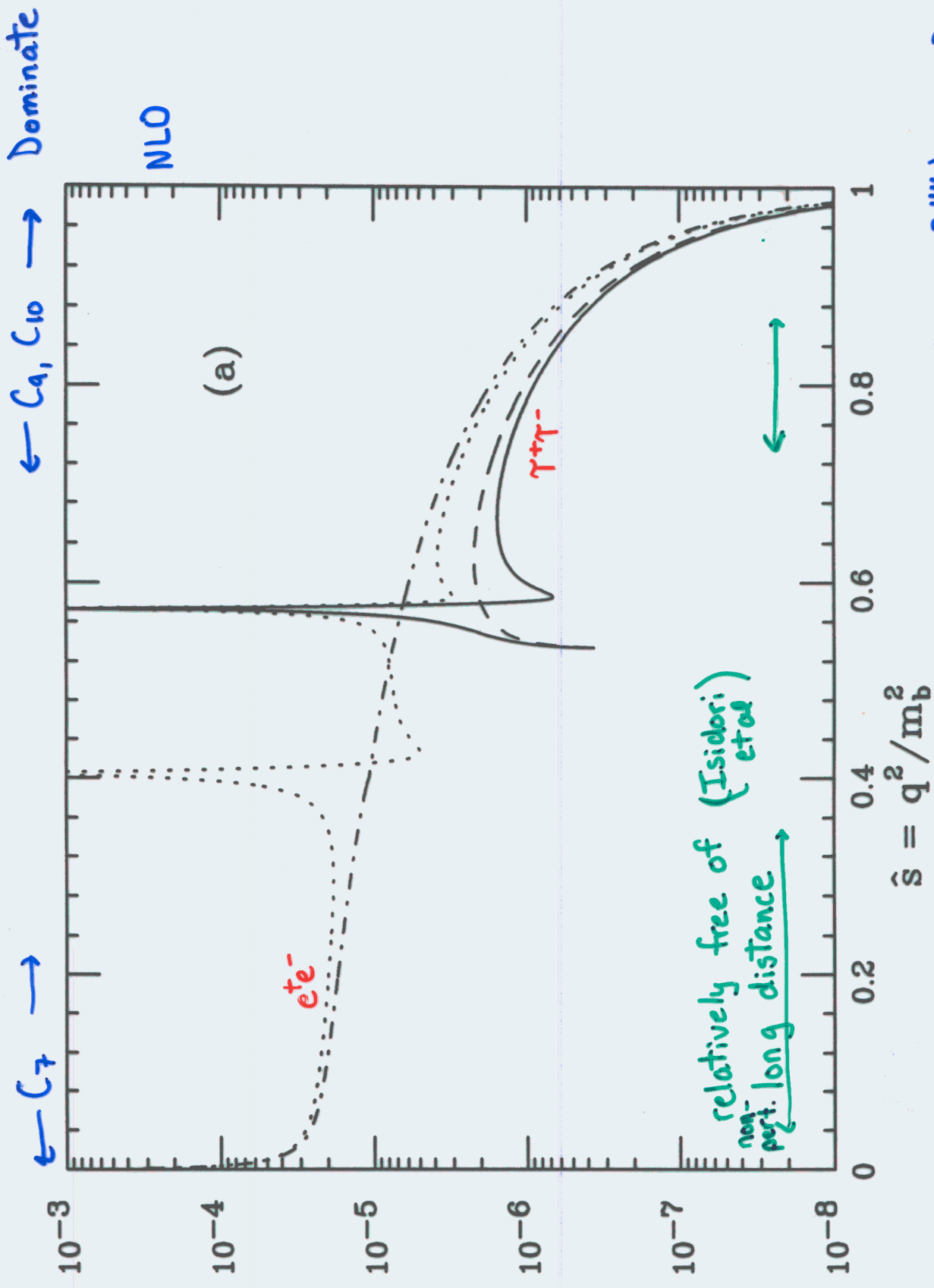
$1/m_c$

Buchalla, Isidori, Rey
Chen, Rupak, Savage

A_{FB} to NNLL

Ghinculov, Hurth, Isidori, Yao
Asatrian, Bieri, Greub,
Hovhannishyan

Tour de Force Effort #2!



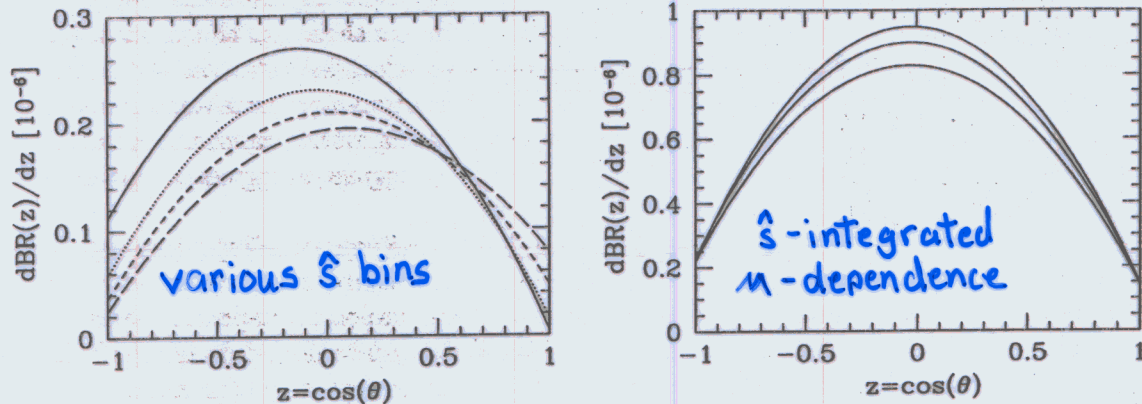
$$B(B \leftarrow X_3, Y_4) = (E \cdot E_{H^+} H^- O_{S^+}) \times 10^{-4}$$

$$B(B \rightarrow X_{S\bar{c}te.}) = (6.25 \pm 0.7) \times 10^{-6}$$

$$B(B \rightarrow X_{S+M}) = (4.15 \pm 1.0) \times 10^{-6}$$

NNLL Corrections

Angular Distributions:



Asatrian et al
hep-ph/
0209006

$$\hat{s} = q_b^2/m_b^2$$

FIG. 7. Left frame: NNLL branching ratio differential in $z = \cos \theta$ for four bins in \hat{s} . Bin 1: $0.05 \leq \hat{s} \leq 0.10$ (solid); bin 2: $0.10 \leq \hat{s} \leq 0.15$ (dotted); bin 3: $0.15 \leq \hat{s} \leq 0.20$ (short-dashed); bin 4: $0.20 \leq \hat{s} \leq 0.25$ (long-dashed). $m_c^{\text{pole}}/m_b^{\text{pole}} = 0.29$ and $\mu = 5$ GeV.
Right frame: NNLL branching ratio differential in $z = \cos \theta$. \hat{s} is integrated in the interval $0.05 \leq \hat{s} \leq 0.25$. The curves correspond to $\mu = 2.5$ GeV (lowest), 5.0 GeV (middle) and 10.0 GeV (uppermost). $m_c^{\text{pole}}/m_b^{\text{pole}} = 0.29$.

Forward- Backward Asymmetry

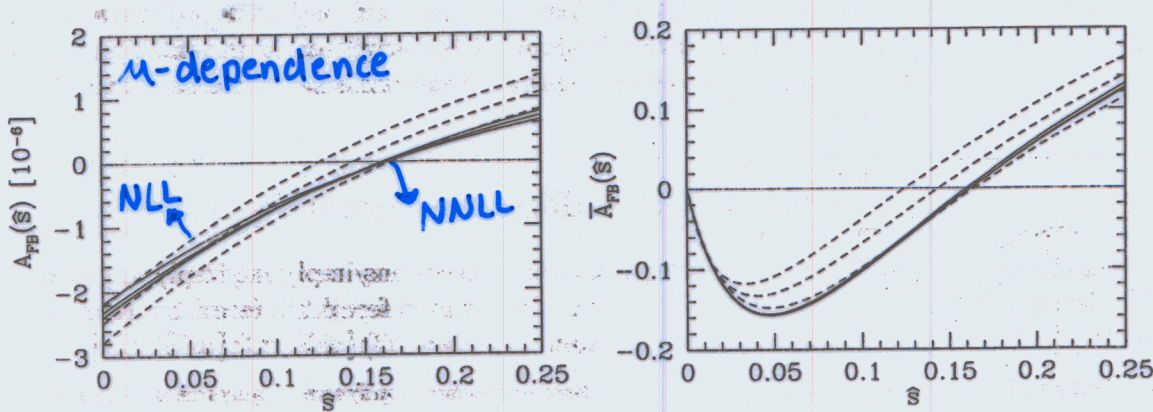


FIG. 4. Left frame: Unnormalized forward-backward asymmetry $A_{FB}(\hat{s})$. The three solid lines show the NNLL prediction for $\mu = 2.5, 5.0, 10.0$ GeV, respectively. The corresponding curves in NLL approximation are shown by dashed lines. Right frame: Normalized forward-backward asymmetry $\bar{A}_{FB}(\hat{s})$. The lines have the same meaning as in the left frame. $m_c/m_b = 0.29$.

Theory + Data Comparison

SM predictions at NNLO accuracy & Comparison with Data
 (all in units of 10^{-6})

[A.A., Lunghi, Greub, Hiller, DESY 01-217; hep-ph/0112300]

Ali ICHEP 02

Decay Mode	Theory (SM)	BELLE	BABAR
$B \rightarrow K\ell^+\ell^-$	0.35 ± 0.12	$0.75^{+0.25}_{-0.21} \pm 0.09$ $0.58^{+0.17}_{-0.15} \pm 0.06$	$0.84^{+0.30}_{-0.24} \pm 0.10$ $0.78^{+0.24}_{-0.20} \pm 0.11$ $1.68^{+0.68}_{-0.58} \pm 0.21$
$B \rightarrow K^*e^+e^-$	1.58 ± 0.52	< 5.1	
$B \rightarrow K^*\mu^+\mu^-$	1.2 ± 0.4	< 3.0	< 3.0 ; weighted $e^+e^-,\mu^+\mu^-$
$B \rightarrow X_s\mu^+\mu^-$	4.15 ± 1.0	$8.9^{+2.3+1.6}_{-2.1-1.7}$ $7.9^{+2.4}_{-1.5} \pm 2.0$	-
$B \rightarrow X_se^+e^-$	6.9 ± 0.70	< 11.0 $5.0^{+2.3}_{-1.7} \pm 4.2$	-
$B \rightarrow X_s\ell^+\ell^-$	5.6 ± 0.9	$7.1 \pm 1.6^{+1.6}_{-1.2}$ $6.1 \pm 1.4^{+1.3}_{-1.1}$	-

① S. Nishida (ICHEP 2002)

② J. Richman (ICHEP 2002)

- Experiments + SM in good accord;
- Improved precision crucial to disentangle NP effects

Global Fit to the Wilson Coefficients

Ingredients: • $B(B \rightarrow X_s \gamma)$ - Flat 10% systematic error

- Divide ll spectrum
into 9 bins
stat. errors only
{randomly
fluctuated}
- M_{ll} Distribution in $B \rightarrow X_s l^+ l^-$
 - $l^+ l^-$ Forward-Backward Asymmetry
in $B \rightarrow X_s l^+ l^-$ [Ali '89]
 - γ Polarization Asymmetry in $B \rightarrow X_s \gamma^+ \gamma^-$ [JLH '95]

Perform Theorist's Monte Carlo - χ^2 fit to simulated
data (assuming SM)

⇒ Determines magnitude + sign of
 $C_7(\mu)$, $C_9(\mu)$, $C_{10}(\mu)$!

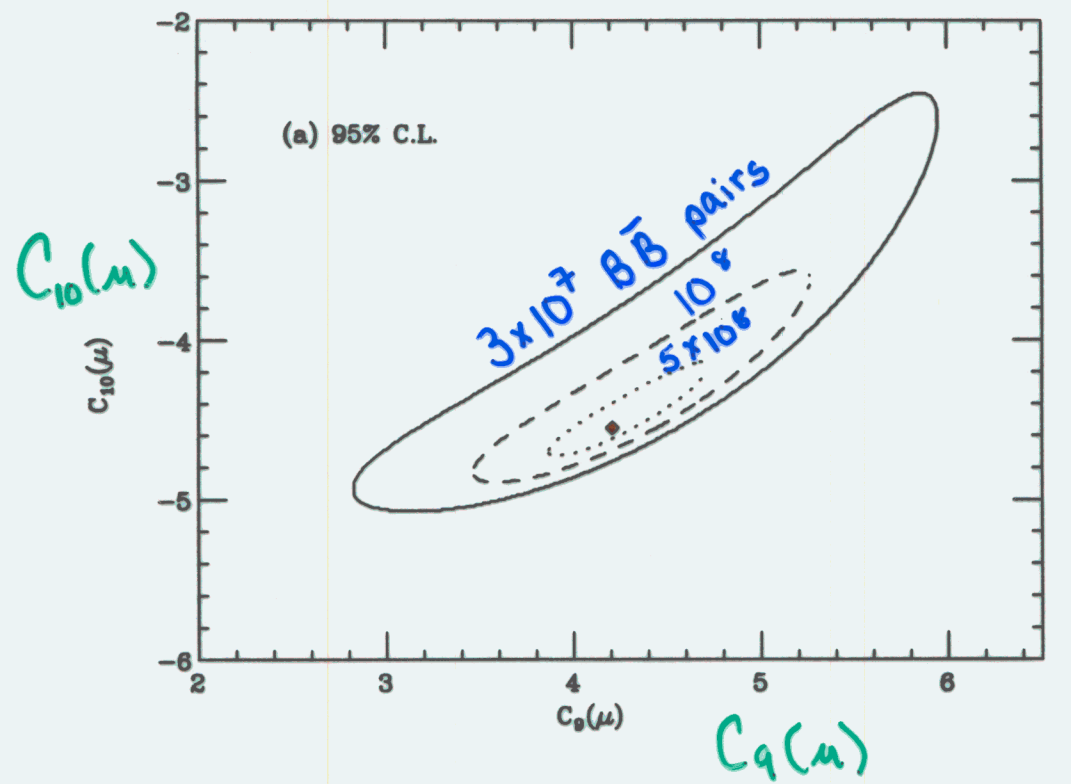
Offers precision test of New Physics

Global Fit To Wilson Coefficients

JLH, Wells

'96

hep-ph/9610323

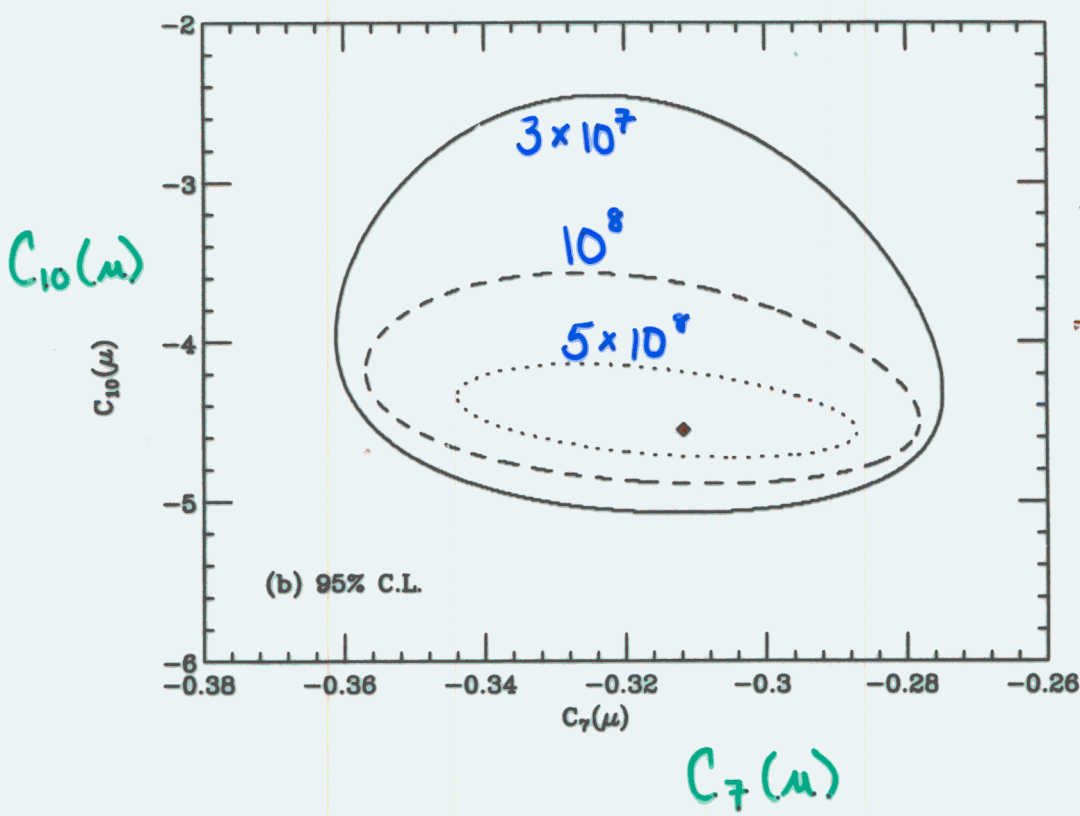


SM:

$$C_7(\mu) = -0.31 \begin{matrix} -0.06 \\ +0.03 \end{matrix}$$

$$C_9(\mu) = 4.2 \begin{matrix} +0.3 \\ -0.4 \end{matrix}$$

$$C_{10}(\mu) = -4.55$$



Event rate converter

<u>B\bar{B}'s</u>	<u>see /smu</u>
3×10^7	225
10^8	750
5×10^8	3780

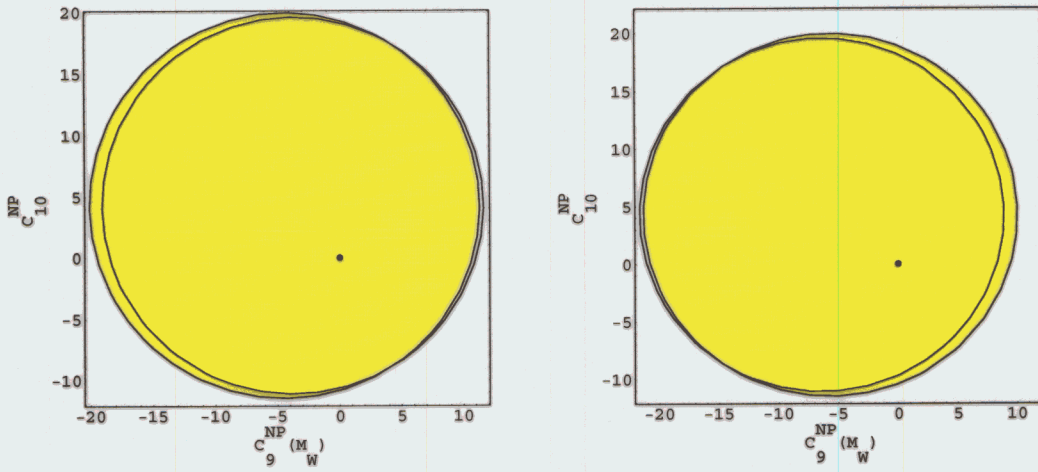
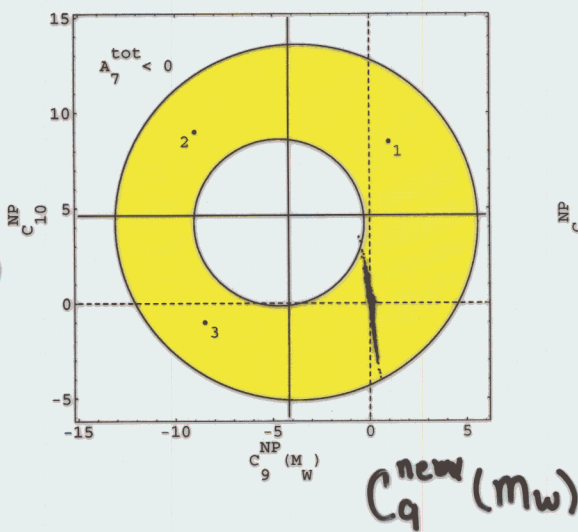


Figure 9: **NNLO Case.** Constraints in the $[C_9^{NP}(\mu_W), C_{10}^{NP}]$ plane that come from the 90%CL BELLE constraint $\mathcal{B}(B \rightarrow K^* e^+ e^-) \leq 5.1 \times 10^{-6}$. See Fig. 4 for further details.

Summary of all Constraints:

$A_{FB} < 0$

$C_{10}^{\text{new}}(\mu_W)$



$A_{FB} > 0$

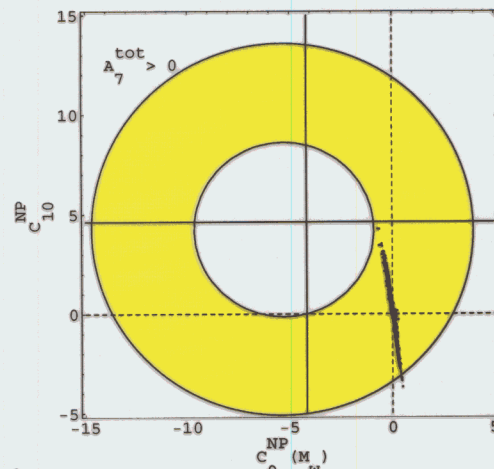


Figure 10: **NNLO Case.** Superposition of all the constraints. The plots correspond to the $A_7^{\text{tot}}(2.5 \text{ GeV}) < 0$ and $A_7^{\text{tot}}(2.5 \text{ GeV}) > 0$ case, respectively. The points are obtained by means of a scanning over the EMFV parameter space and requiring the experimental bound from $B \rightarrow X_s \gamma$ to be satisfied.

New Physics Effects in the Global Fit:

1) Determined $C_i = C_i^{\text{sm}}$ with good χ^2

\Rightarrow New Physics is decoupled

2) Good χ^2 , but $C_i \neq C_i^{\text{sm}}$

\Rightarrow New Physics present in loops

3) Large χ^2 for best-fit

\Rightarrow Extended Operator Basis

Examples: Left-Right Symmetric Model
Additional 4-Fermi interactions

Rizzo

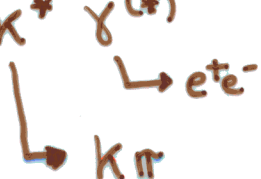
C.S. Kim et al

Tests of Right-handed interactions:

• Λ polarization in $\Lambda_b \rightarrow \Lambda + \gamma$

Mannel, Recksiegel

• Angular correlations in $B \rightarrow K^* \gamma^{(*)}$



Grossman, Pirjol

Effective Field Theory Approach to mFV

Ambrosio et al
hep-ph/0207036

Construct complete set of gauge + CP invariant dimension-6 operators.

Scale operators as: $\pm \frac{\Theta_i}{\Lambda^2}$, where $\Lambda = \text{New Physics scale}$

Minimally flavour violating dimension six operator

$$\begin{aligned} \mathcal{O}_0 &= \frac{1}{2} (\bar{Q}_L \lambda_{FC} \gamma_\mu Q_L)^2 \\ \mathcal{O}_{F1} &= H^\dagger (\bar{D}_R \lambda_d \lambda_{FC} \sigma_{\mu\nu} Q_L) F_{\mu\nu} \\ \mathcal{O}_{G1} &= H^\dagger (\bar{D}_R \lambda_d \lambda_{FC} \sigma_{\mu\nu} T^a Q_L) G_{\mu\nu}^a \\ \mathcal{O}_{\ell 1} &= (\bar{Q}_L \lambda_{FC} \gamma_\mu Q_L) (\bar{L}_L \gamma_\mu L_L) \\ \mathcal{O}_{\ell 2} &= (\bar{Q}_L \lambda_{FC} \gamma_\mu \tau^a Q_L) (\bar{L}_L \gamma_\mu \tau^a L_L) \\ \mathcal{O}_{H1} &= (\bar{Q}_L \lambda_{FC} \gamma_\mu Q_L) (H^\dagger i D_\mu H) \\ \mathcal{O}_{q5} &= (\bar{Q}_L \lambda_{FC} \gamma_\mu Q_L) (\bar{D}_R \gamma_\mu D_R) \end{aligned}$$

main observables

$$\begin{aligned} \epsilon_K, \Delta m_{B_d} \\ B \rightarrow X_s \gamma \\ B \rightarrow X_s \gamma \\ B \rightarrow (X) l \bar{l}, K \rightarrow \pi \nu \bar{\nu}, (\pi) l \bar{l} \\ B \rightarrow (X) l \bar{l}, K \rightarrow \pi \nu \bar{\nu}, (\pi) l \bar{l} \\ B \rightarrow (X) l \bar{l}, K \rightarrow \pi \nu \bar{\nu}, (\pi) l \bar{l} \\ B \rightarrow K \pi, \epsilon'/\epsilon, \dots \end{aligned}$$

Λ [TeV]

$$\begin{array}{cc} - & + \\ 6.4 & 5.0 \\ 9.3 & 12.4 \\ 2.6 & 3.5 \\ 3.1 & 2.7 & * \\ 3.4 & 3.0 & * \\ 1.6 & 1.6 & * \\ \sim 1 & & \end{array}$$

$B \rightarrow X_s \gamma$

Constraints:

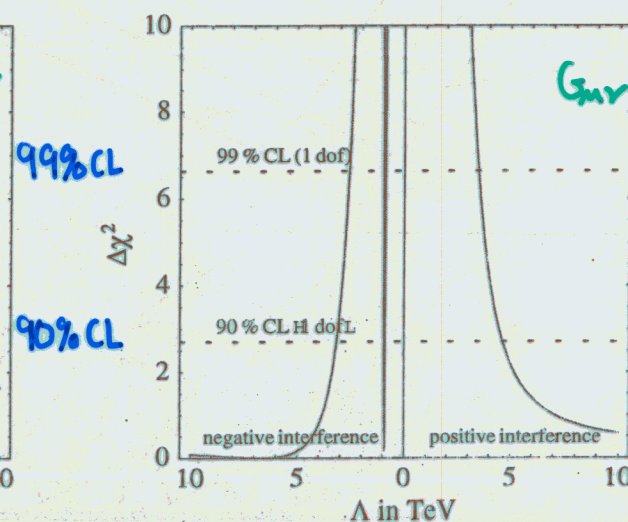
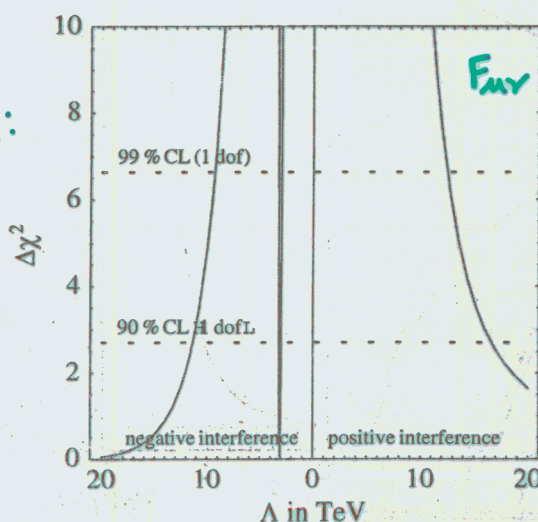


Figure 2: Bounds on the scale of the operators \mathcal{O}_{F1} (left) and \mathcal{O}_{G1} (right) from $B \rightarrow X_s \gamma$.

$B \rightarrow X_s \gamma$ Constraints

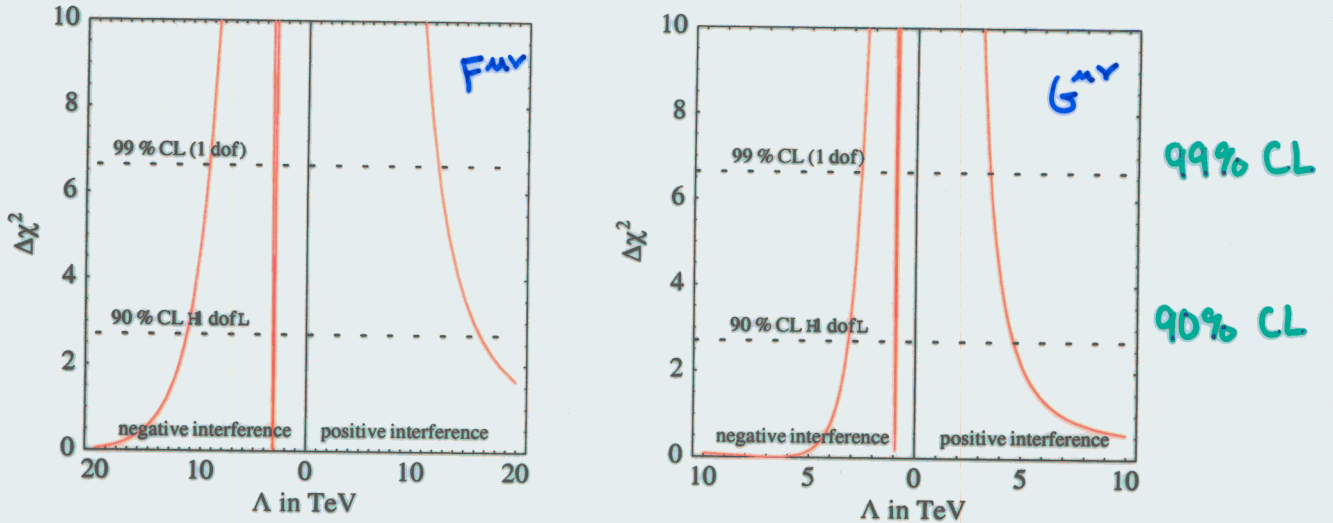


Figure 2: *Bounds on the scale of the operators \mathcal{O}_{F1} (left) and \mathcal{O}_{G1} (right) from $B \rightarrow X_s \gamma$.*

result [19]

$$\mathcal{B}(K^+ \rightarrow \pi^+ \nu \bar{\nu}) = \left(1.57 \pm \frac{1.75}{0.82} \right) \times 10^{-10}. \quad (30)$$

leads to the 99% CL limit

$$-4.8 < C_{\nu \bar{\nu}} / C_{\nu \bar{\nu}}^{\text{SM}} < 4.0. \quad (31)$$

These bounds are still rather weak, corresponding to effective scales of the new physics operator around 1 TeV, nonetheless they already imply significant bounds on $\mathcal{B}(K_L \rightarrow \pi^0 \nu \bar{\nu})$ and $\mathcal{B}(B \rightarrow X_s \nu \bar{\nu})$, as shown in table 3 (see also ref. [20]). In few years, at the end of the E949 experiment, assuming that the central value of $\mathcal{B}(K^+ \rightarrow \pi^+ \nu \bar{\nu})$ will move towards the SM prediction, we can expect to probe Λ from this observable up to about 3 TeV, a sensitivity comparable to the one of electroweak precision data on the corresponding flavour-diagonal terms. At the end of the CKM experiment, with a 10% measurement of this branching ratio, the search on Λ could be pursued up to above 5 TeV. As illustrated in fig. 4, a sensitivity above 10 TeV could in principle be reached by a measurement of $\mathcal{B}(K_L \rightarrow \pi^0 \nu \bar{\nu})$ with a precision of few percent around the SM value, since this rate is free from the theoretical uncertainty due to charm contributions.

The most interesting constraint on pure-leptonic decays is provided by $K_L \rightarrow \mu^+ \mu^-$. The branching ratio of this decay is measured very precisely; however, this mode receives also a large long-distance amplitude by the two-photon intermediate state. Actually short- and long-distance dispersive parts cancel each other to a good extent, since the total $K_L \rightarrow \mu^+ \mu^-$ rate is almost saturated by the absorptive two-photon contribution. Taking into account the recent experimental result on $\mathcal{B}(K_L \rightarrow \mu^+ \mu^-)$ [21] and following the analyses of the long-distance amplitude in [22], we shall impose the conservative upper bound

$$\mathcal{B}(K_L \rightarrow \mu^+ \mu^-)^{\text{short}} \leq 3.0 \times 10^{-9}, \quad (32)$$

that we shall treat as an absolute limit. Employing the SM expression of $\mathcal{B}(K_L \rightarrow \mu^+ \mu^-)^{\text{short}}$ [3] and taking into account the uncertainty of the CKM fit, this information can be translated

Supersymmetry: General Features

Very many authors

$B \rightarrow X_s \gamma$: Large restrictions!

particularly for large $\tan \beta$, $m < 0$

$B \rightarrow X_s l^+ l^-$: Smaller contributions to rate
Deviations in Asymmetries

$B_s \rightarrow l^+ l^-$: Large contributions from
Higgs exchange for
large $\tan \beta$

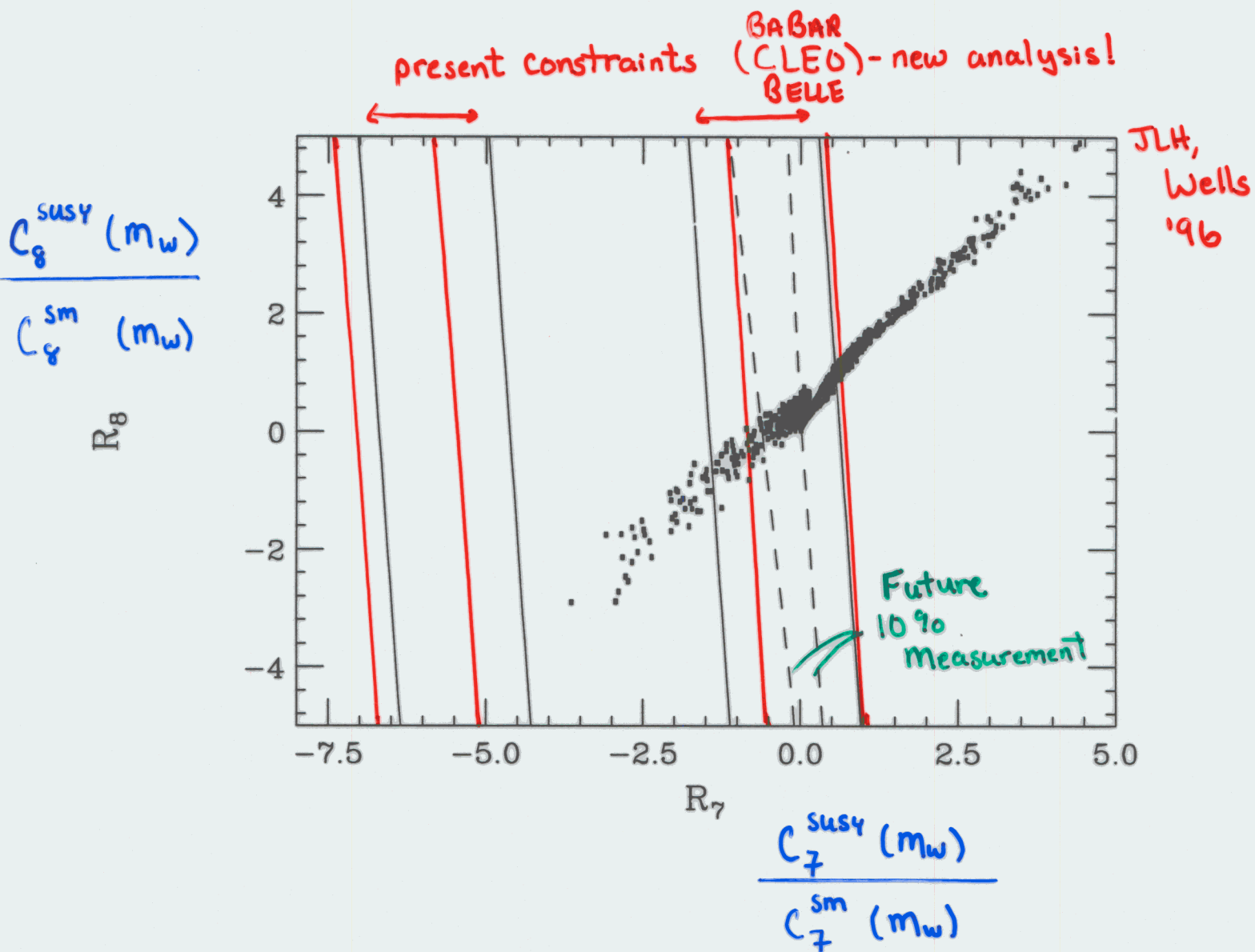
Babu, Kolda

Distinct patterns emerge for various SUSY-breaking scenarios!

Possible (if lucky) to learn about SUSY breaking from rare decays!

SUSY + Unification + Radiative Breaking = mssm

Generate 2000 points consistent with SUSY scales
above LEP II + Tevatron reach



Pick $\tilde{m}_0, \tilde{m}_{1/2}, A_0, \text{sign}(\mu), \tan\beta$ at GUT scale
+ RGE evolve to EW/TeV scale

Constraints on 2-d SUSY parameter plane

MSUGRA

$$\tan\beta = 10, A_0 = 0, \mu > 0$$

Baer et al
hep-ph/0205325

Common gaugino mass

Contours of $B \rightarrow X_s \gamma$ in 10^{-4}

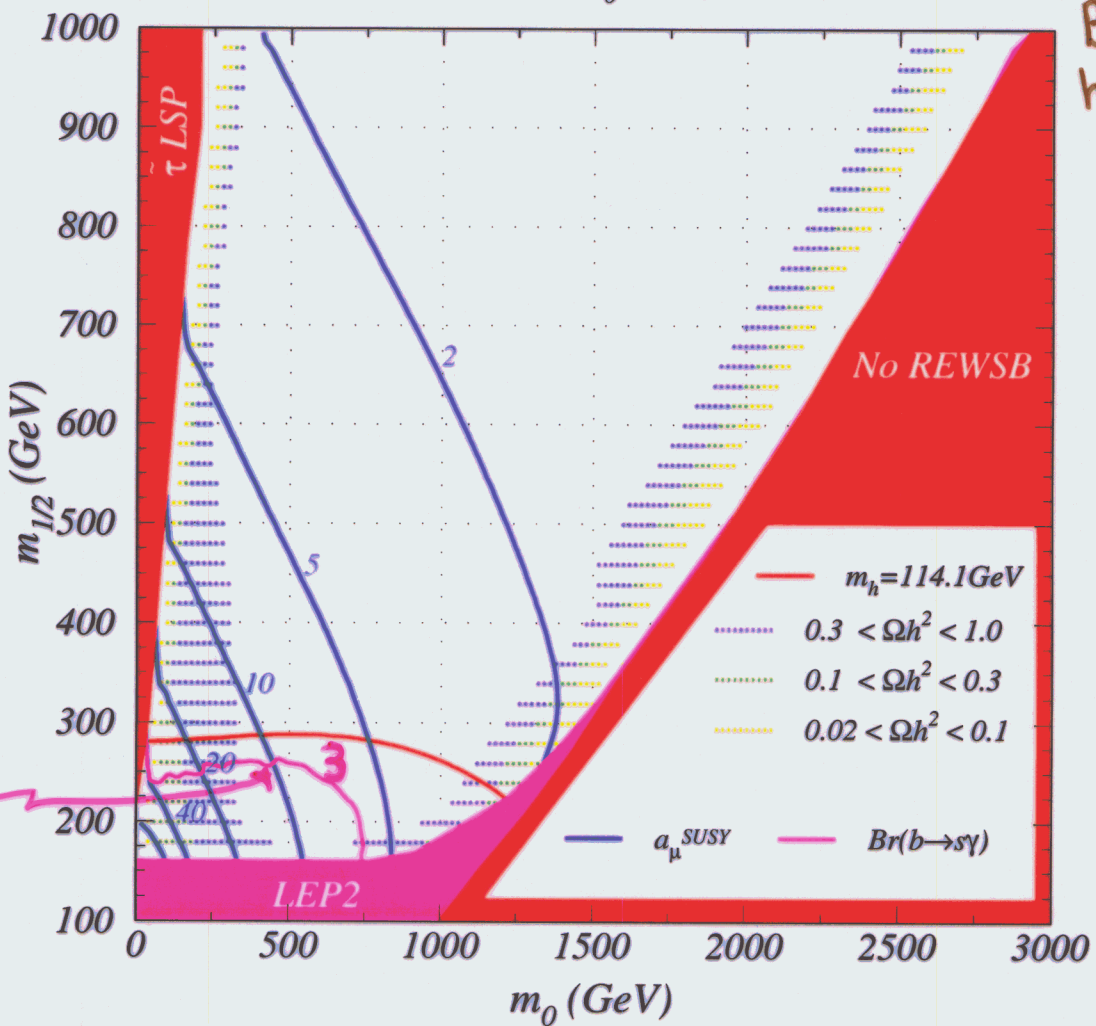


Figure 2: Same as Fig. 1, but for $\mu > 0$.

enhanced neutralino annihilation to $b\bar{b}$ and $\tau\bar{\tau}$ at large $\tan\beta$. Both lighter values of $m_{\tilde{\tau}_1}$ and $m_{\tilde{b}_1}$ and also large τ and b Yukawa couplings at large $\tan\beta$ enhance these t -channel annihilation rates through virtual staus and sbottoms. Unfortunately, the region excluded by $BF(b \rightarrow s\gamma)$ and by δa_μ (even with the conservative constraint of Ref.[43]) also expands, and most of the cosmologically preferred region is again ruled out. As before, we are left with the corridors of stau co-annihilation and the focus point scenario as the only surviving regions.

The corresponding plot is shown for $\tan\beta = 30$ but $\mu > 0$ in Figure 4. In this case, the magenta contours of $BF(b \rightarrow s\gamma)$ correspond to 2 and 3×10^{-4} . Thus, the lower left region is excluded since it leads to too *low* a value of $BF(b \rightarrow s\gamma)$. The δa_μ contours begin

mSUGRA

$\tan\beta = 10, A_0 = 0, \mu < 0$

Baer et al

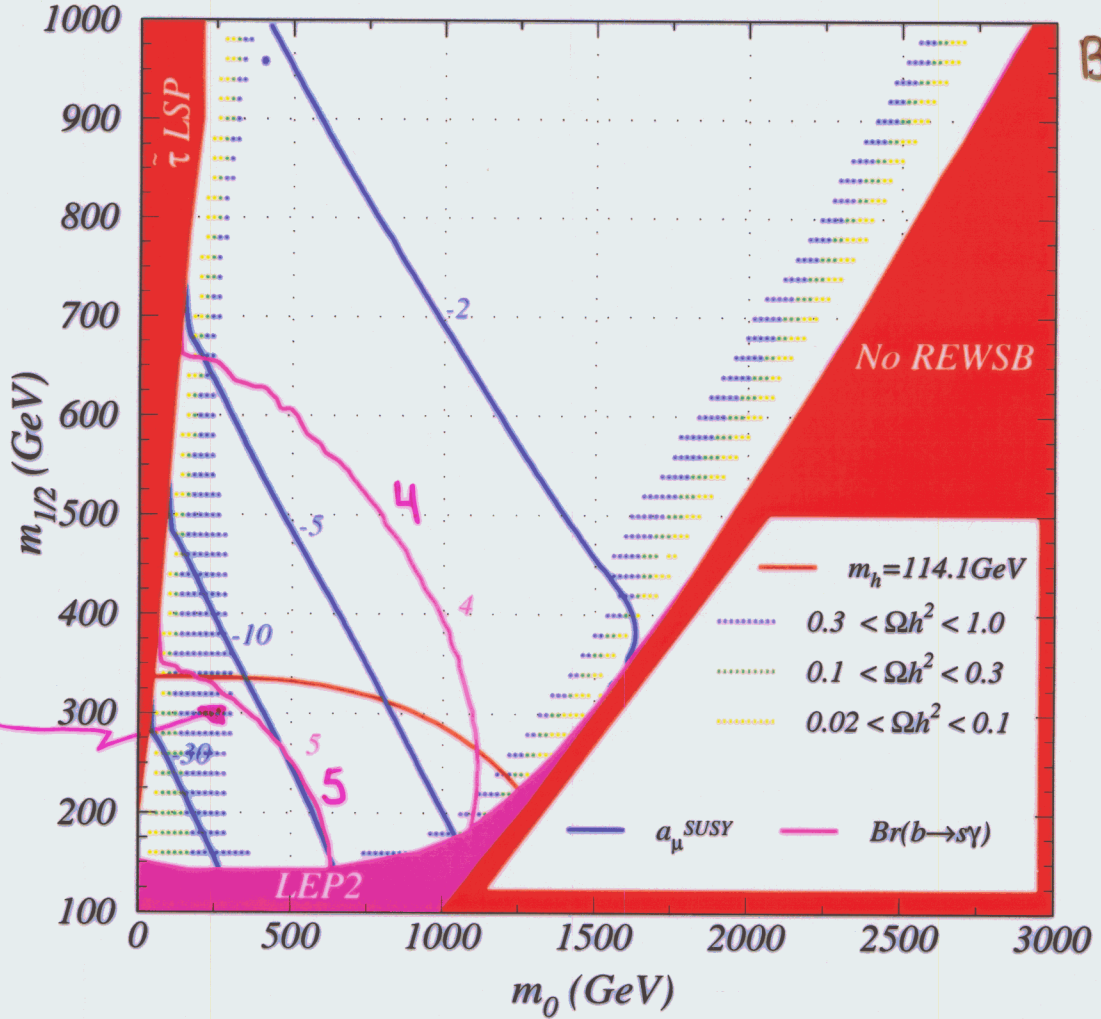


Figure 1: Plot of constraints for the mSUGRA model in the m_0 vs. $m_{1/2}$ plane for $\tan\beta = 10$, $A_0 = 0$ and $\mu < 0$. We show regions of CDM relic density, plus contours of $m_h = 114.1$ GeV, contours of muon anomalous magnetic moment a_μ ($\times 10^{10}$) and contours of $b \rightarrow s\gamma$ branching fraction ($\times 10^4$).

preferred value of neutralino relic density, one must again live in the stau co-annihilation region, or the focus point region. A final possibility is to be in the slepton annihilation region, but then the value of m_h should be slightly beyond the LEP2 limit; in this case, a Higgs boson signal may be detected in Run 2 of the Fermilab Tevatron[51].

We next turn to the m_0 vs. $m_{1/2}$ plane for $\tan\beta = 30$ and $\mu < 0$. The gray region in the bottom left corner of the plot is excluded because $m_{\tilde{\tau}_1}^2 < 0$. In this case, the area of the green region of relic density in the lower-left has expanded considerably owing to

mSUGRA

$\tan\beta = 45, A_0 = 0, \mu < 0$

Baer et al

Contours of
 $B \rightarrow X_s \gamma$

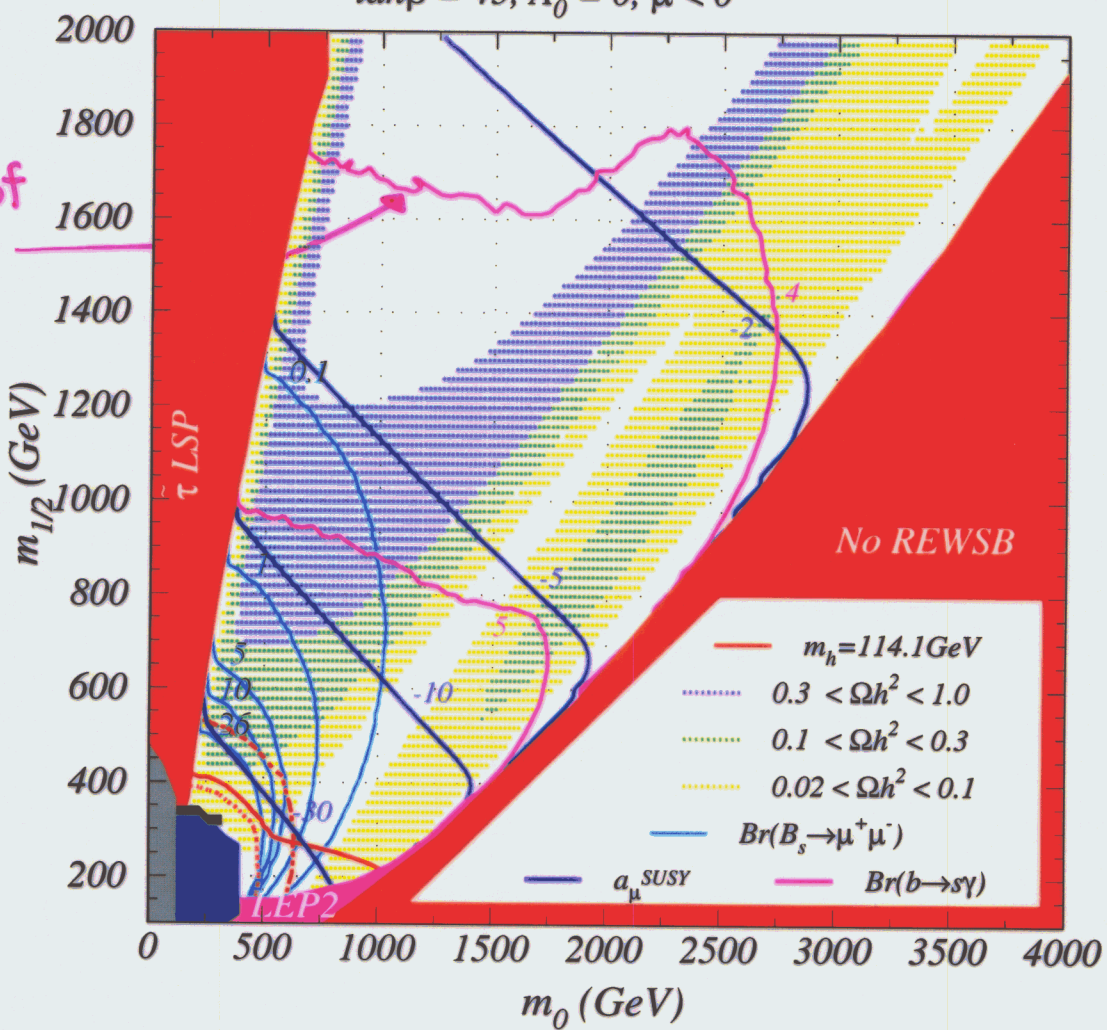


Figure 5: Same as Fig. 1, but for $\tan\beta = 45$ and $\mu < 0$. The inner and outer red dashed lines are contours of $m_A = 100$ and $m_A = 200$ GeV, respectively.

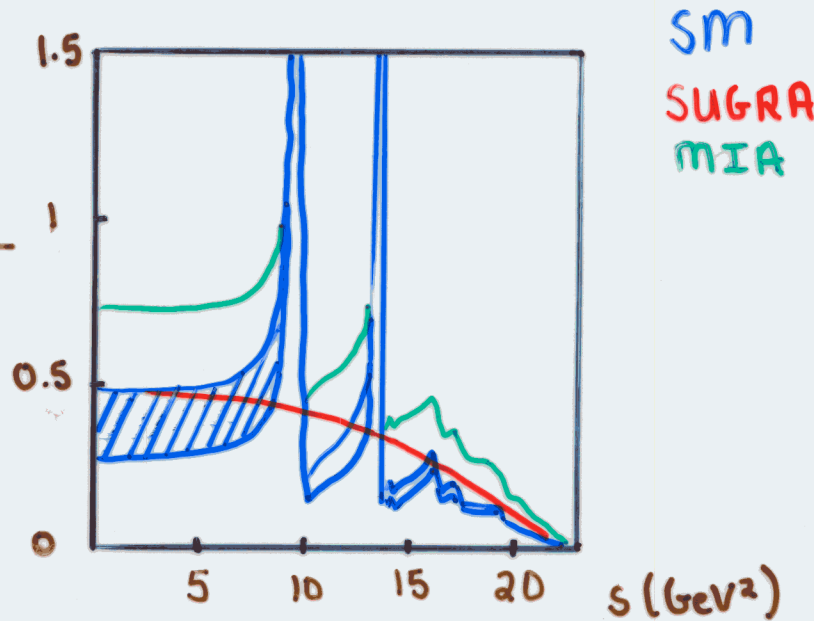
- 1. annihilation through t -channel slepton exchange (low m_0 and $m_{1/2}$),
- 2. the stau co-annihilation region (very low m_0 but large $m_{1/2}$),
- 3. the focus point region (large m_0 but low to intermediate $m_{1/2}$) and
- 4. the flanks of the neutralino s -channel annihilation via A and H corridor at large $\tan\beta$ when Γ_A and Γ_H are very large.

In previous years, there may have been a preference for region 1. as offering the most natural channel for obtaining a reasonable value of relic density. However, recently much of

Exclusive Branching Fractions

$\frac{d\mathcal{B}(B \rightarrow K\mu\mu)}{ds}$

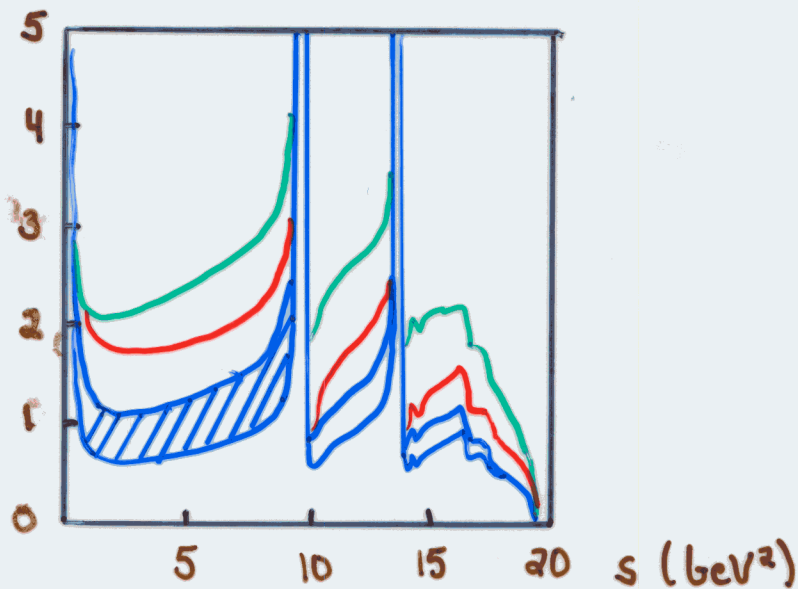
$\times 10^7 \text{ GeV}^{-2}$



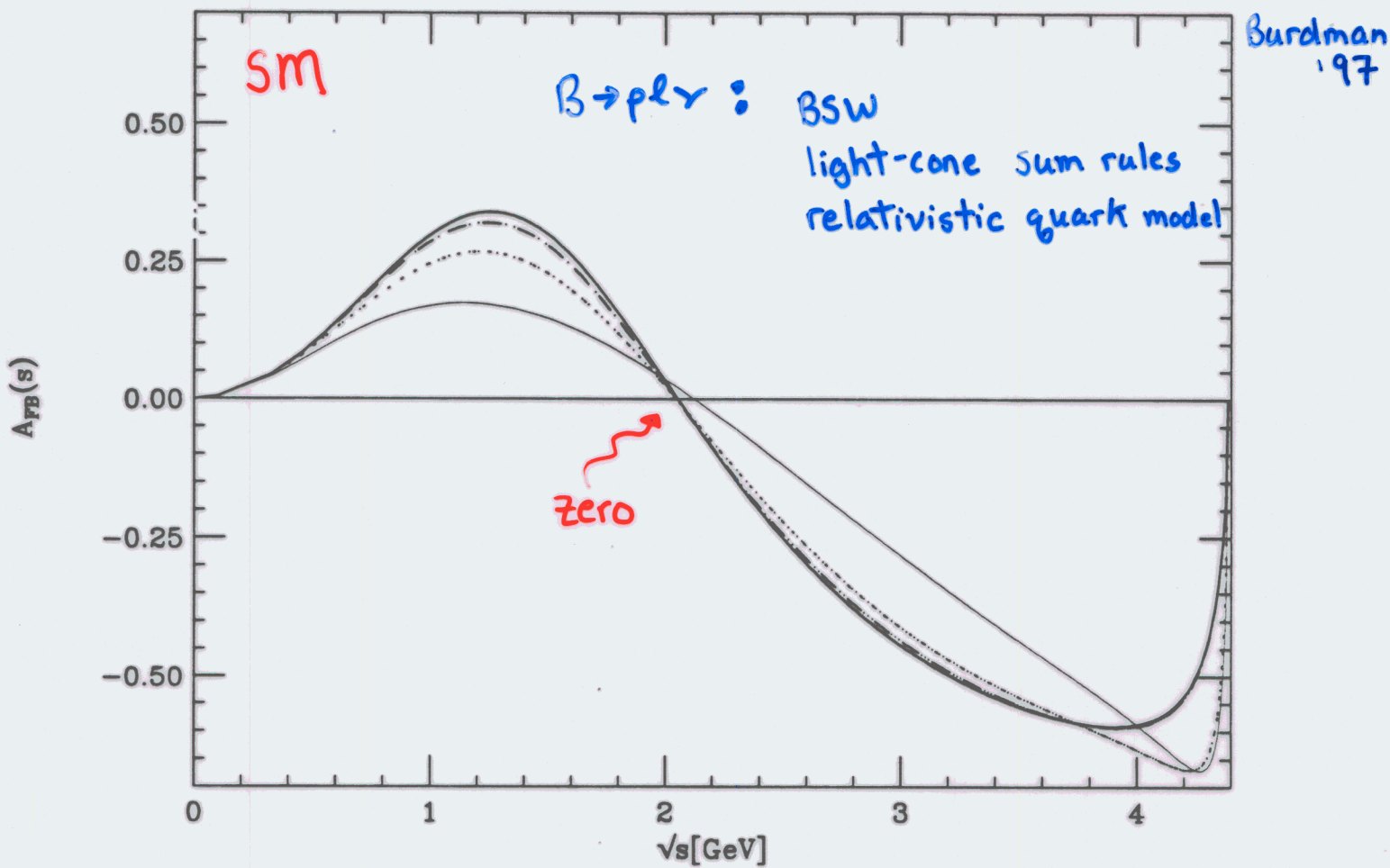
Ali, Ball, Handoko, Hiller

$\frac{d\mathcal{B}(B \rightarrow K^*\mu\mu)}{ds}$

$\times 10^7 \text{ GeV}^{-2}$



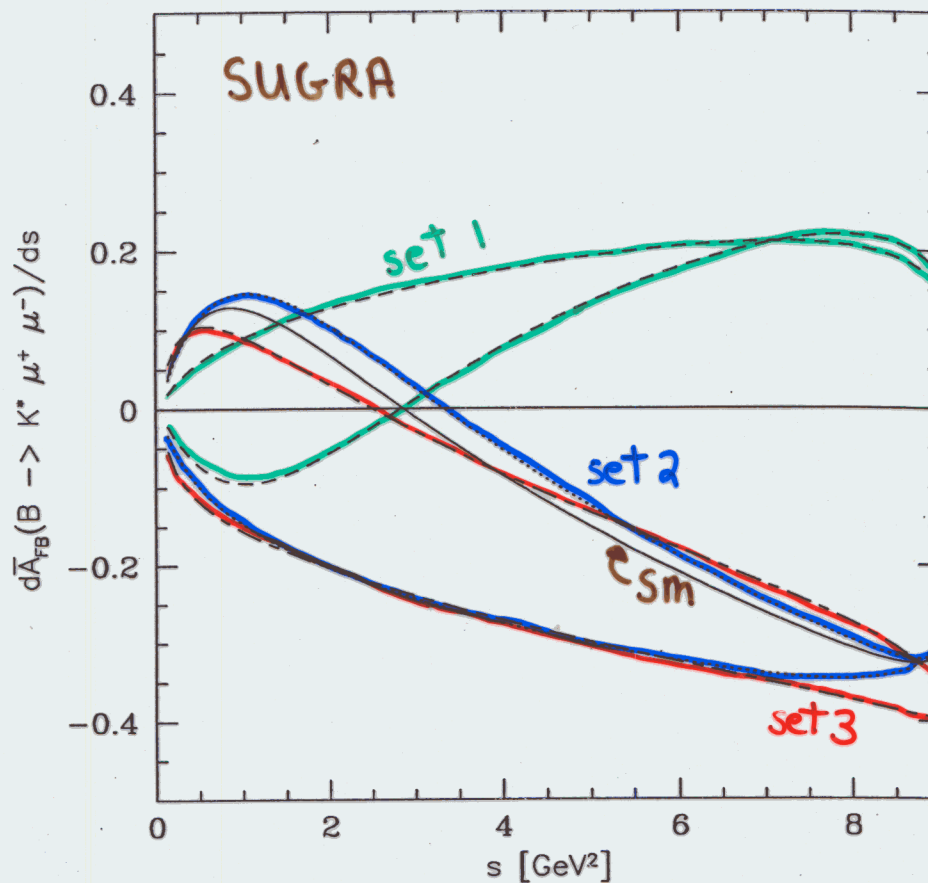
$t\bar{t}e^-$ Forward - Backward Asymmetry for $B \rightarrow K^* e^+ e^-$



Form Factors related to $B \rightarrow pl\gamma$

- Need Accurate Form Factor predictions for exclusive modes!

Position of Asymmetry^{Zero} changes / vanishes with NP!



Clear indication of New Physics!

Correlation between $B_{s,d} \rightarrow ll$ + Δm_s : Large $\tan \beta$

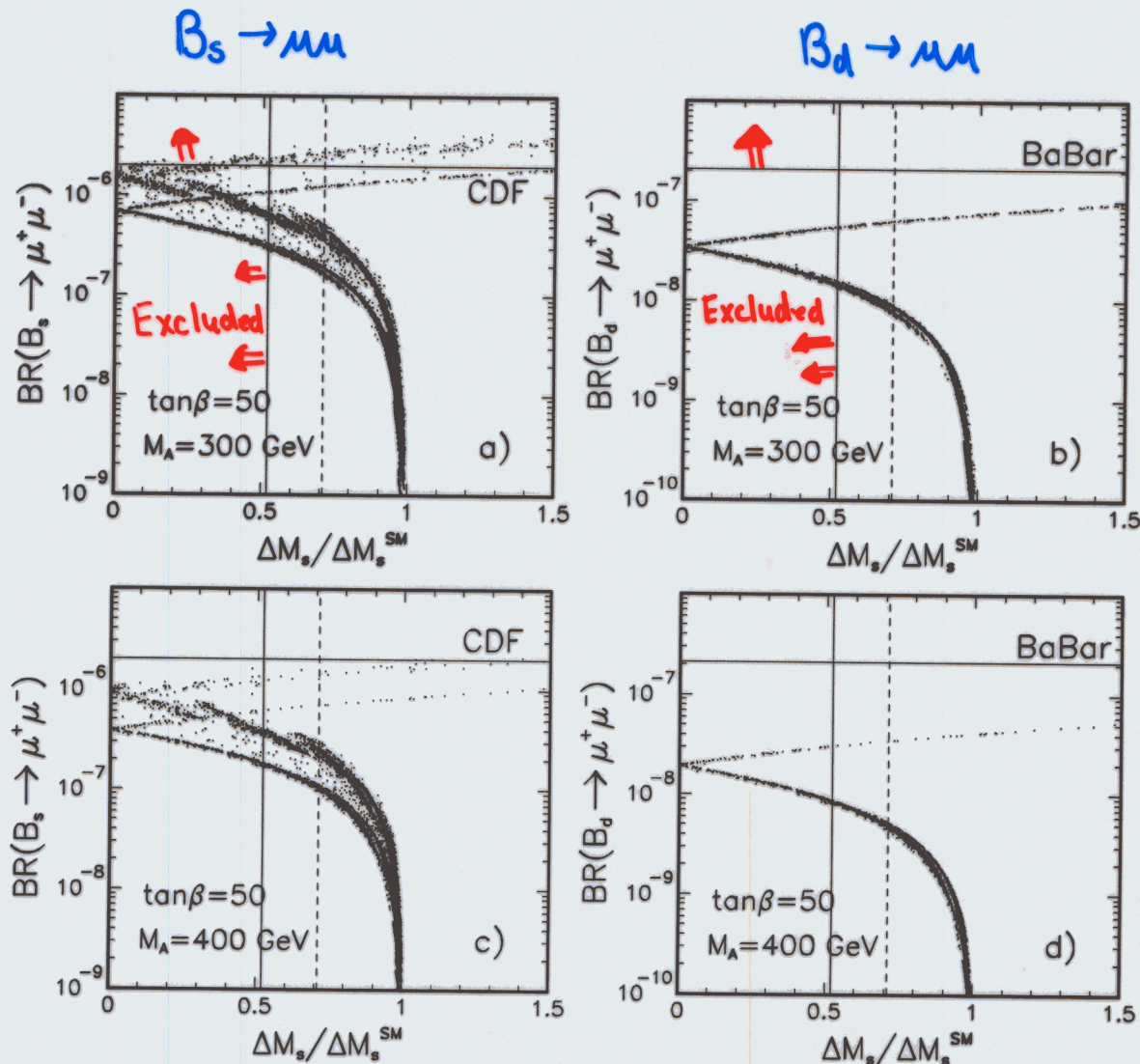


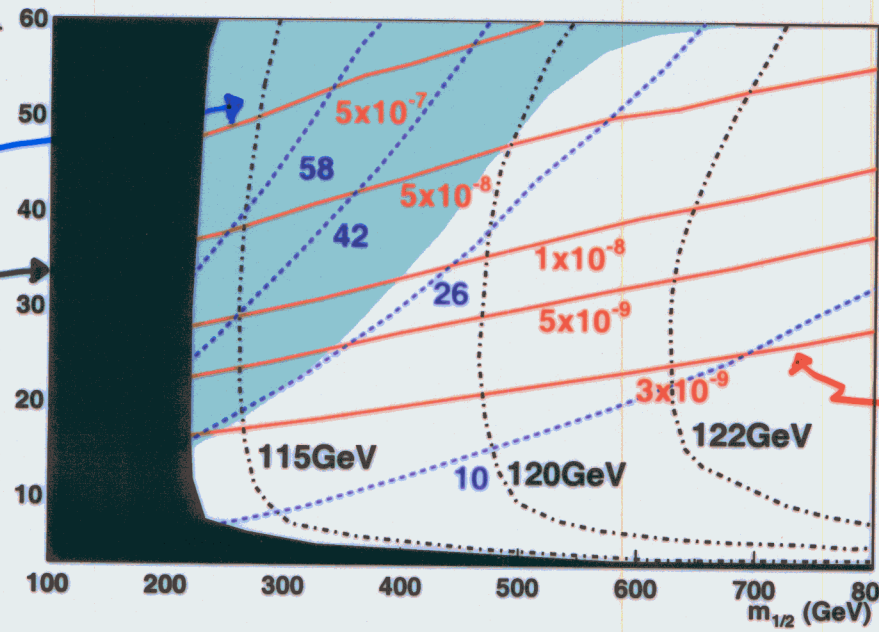
Figure 23: Correlation between $\Delta M_s / (\Delta M_s)^{SM}$ and $B_{s,d}^0 \rightarrow \mu^+ \mu^-$ in the MSSM with flavour violation ruled by the CKM matrix. Lower (upper) branches of points correspond to $0 < 1 + f_s < 1$ ($1 + f_s < 0$). Current experimental bounds: $BR(B_s^0 \rightarrow \mu^+ \mu^-) < 2 \cdot 10^{-6}$ (CDF) [32] and $BR(B_d^0 \rightarrow \mu^+ \mu^-) < 2.1 \cdot 10^{-7}$ (BaBar) [31] are shown by the horizontal solid lines. Solid (dashed) vertical lines show the lower limit on $\Delta M_s / (\Delta M_s)^{SM}$ following from eq. (7.62) with $a = 0.52$ as in ref. [20] ($a = 0.71$ as in [41]).

Patterns from SUSY-breaking mechanisms

Excluded by
 $B \rightarrow X_s \gamma$

Direct
 searches

$\tan \beta$



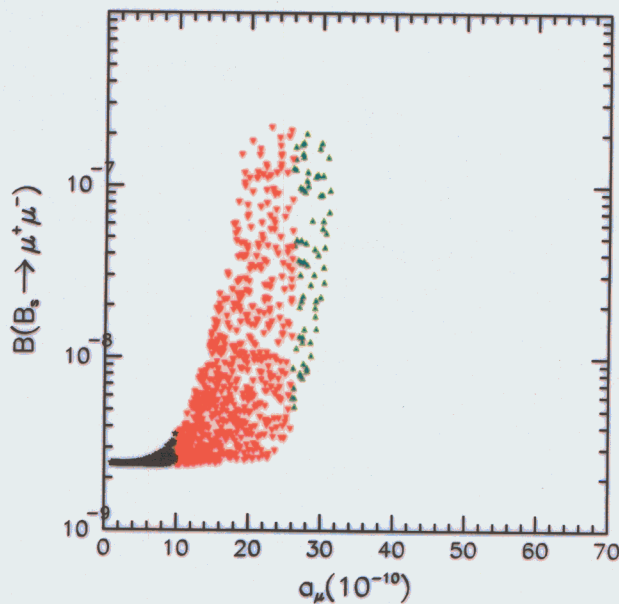
Back, Ko, Song
 hep-ph/0208112

MSUGRA

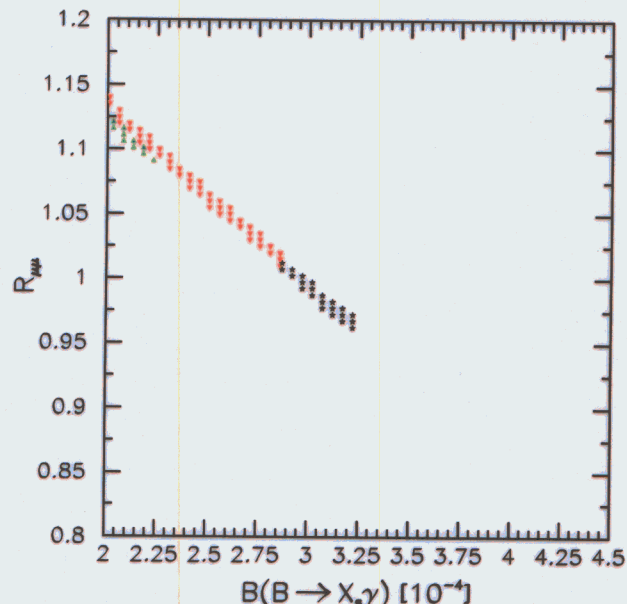
Contours of
 $B_s \rightarrow \mu\mu$

Common gaugino
 mass

FIG. 1: The contour plots for a_μ^{SUSY} in unit of 10^{-10} (in the short dashed curves) and the Br ($B_s \rightarrow \mu^+ \mu^-$) (in the solid curves) in the $(M_{1/2}, \tan \beta)$ plane in the minimal SUGRA model for $m_0 = 300$ GeV and $A_0 = 0$.



(a)



(b)

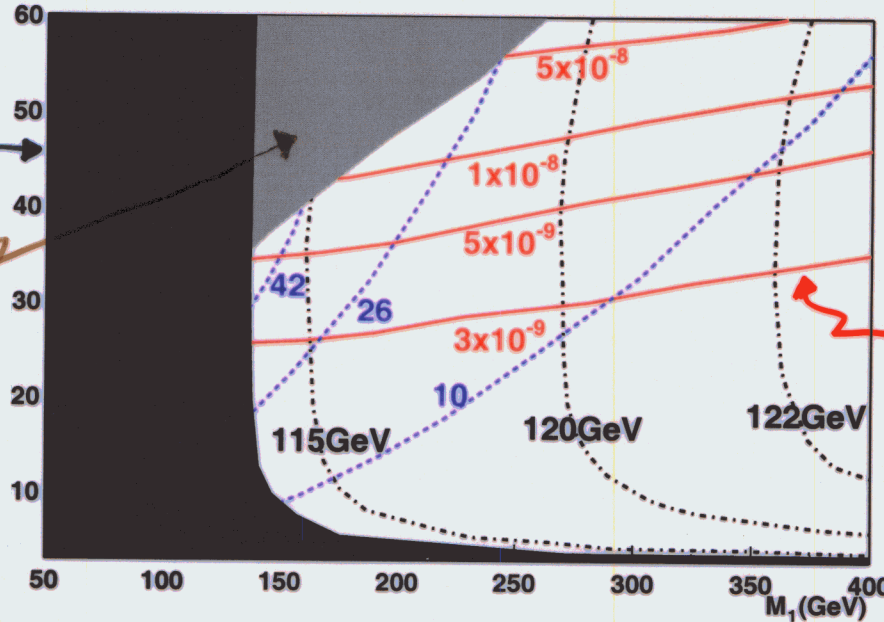
FIG. 2: The correlations between (a) the muon a_μ^{SUSY} and $B(B_s \rightarrow \mu^+ \mu^-)$, and (b) $Br(B \rightarrow X_s \gamma)$ and $R_{\mu\mu}$ in the mSUGRA model with $A_0 = 0$ and $m_0 = 300$ GeV. The regions $a_\mu^{\text{SUSY}} < 10^{-10}$, $10 \times 10^{-10} < a_\mu^{\text{SUSY}} < 26 \times 10^{-10}$, $26 \times 10^{-10} < a_\mu^{\text{SUSY}} < 42 \times 10^{-10}$, $42 \times 10^{-10} < a_\mu^{\text{SUSY}} < 58 \times 10^{-10}$, and $a_\mu^{\text{SUSY}} > 58 \times 10^{-10}$ are represented by the stars (black), the inverted triangles (red), the triangles (green), the squares (blue) and the circles (yellow).

GMSB

Excluded by
Direct Searches

NLSP Bounds

$\tan \beta$



Baek, Ko, Song

Contours of
 $B_s \rightarrow \mu\mu$

Bino mass
parameter

Excluded by

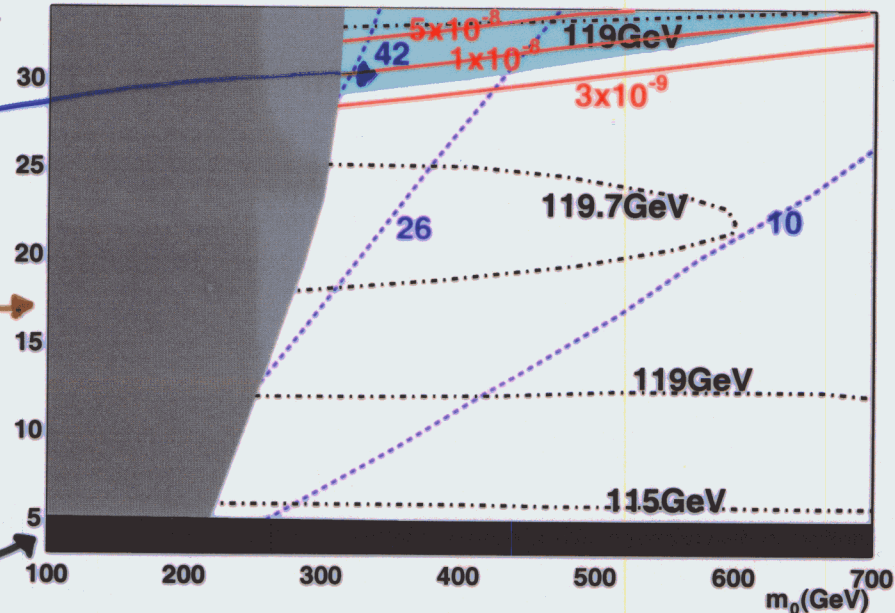
$B \rightarrow \chi_s \gamma$

$\tilde{\tau}$ mass bound

LEP II Higgs
search

AMSB

$\tan \beta$

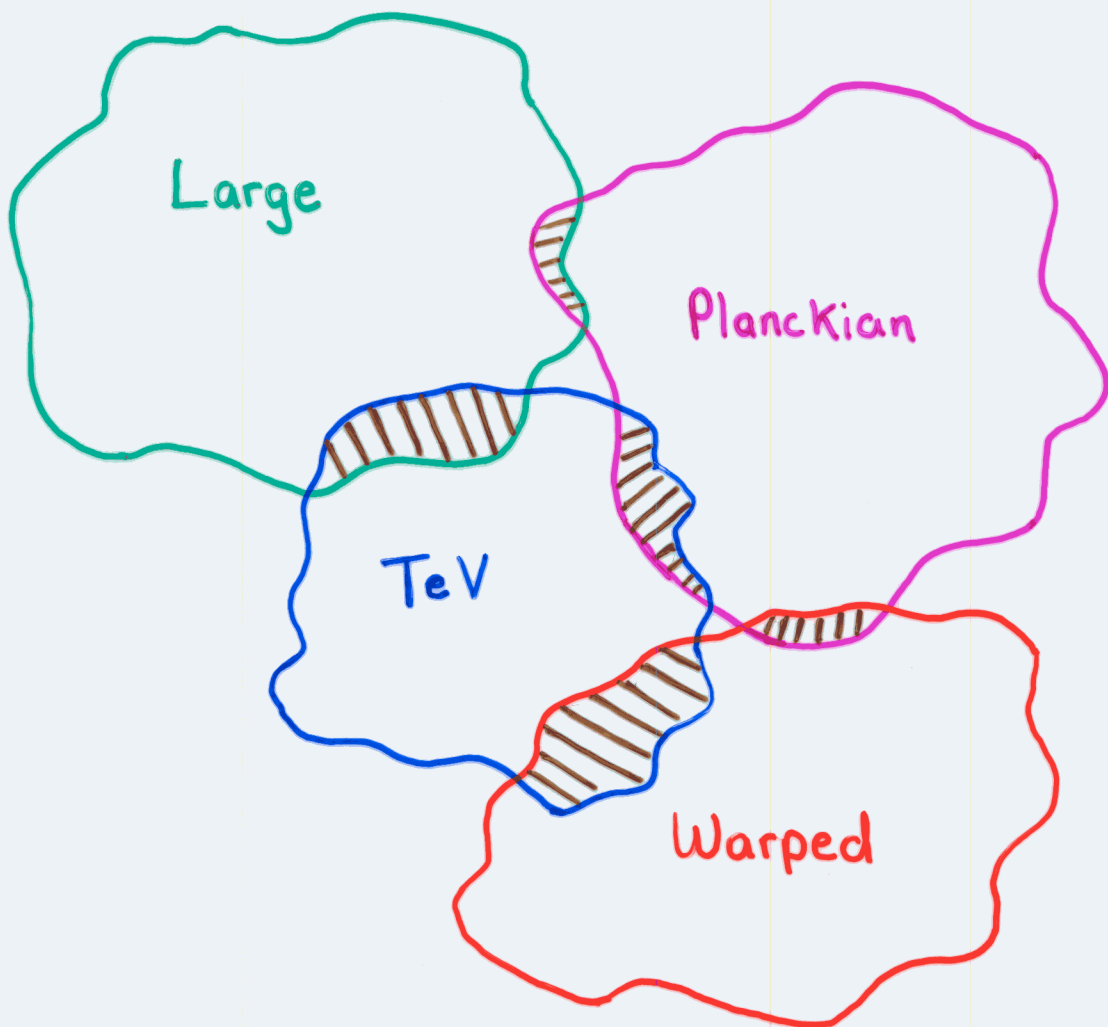


scalar mass
parameter

FIG. 7: The contour plots for a_μ^{SUSY} in unit of 10^{-10} (in the short dashed curves) and the $\text{Br}(B_s \rightarrow \mu^+ \mu^-)$ (in the solid curves) in the $(M_1, \tan \beta)$ plane for the GMSB model with $N_{\text{mess}} = 5$ and $M_{\text{mess}} = 10^{15} \text{ GeV}$. The gray region is excluded by the NLSP mass bound.

FIG. 8: The contour plots for a_μ^{SUSY} in unit of 10^{-10} (in the short dashed curves) and the $\text{Br}(B_s \rightarrow \mu^+ \mu^-)$ (in the solid curves) in the $(m_0, \tan \beta)$ plane for the minimal AMSB scenarios with $M_{\text{aux}} = 50 \text{ TeV}$ and $\mu > 0$.

Extra Dimensions!



Many different types with overlap in features

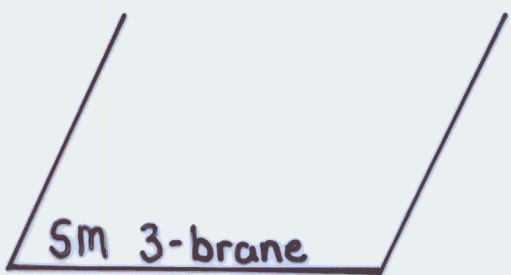
Impact on B physics just starting to be explored !

Physics of Branes: Spatial Dimensional Subspace

Our 3+1-dim subspace = 3-brane

Embedded in $D=3+6+1$ space = bulk

Bulk

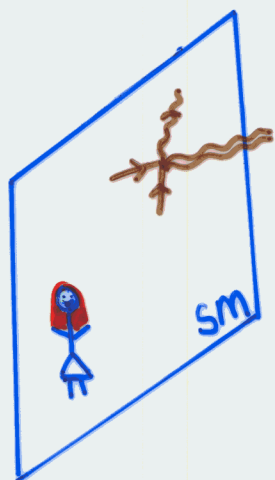


Size & geometry of
bulk can vary

Large Extra Dimensions

Arkani - Hamed,
Dimopoulos, Dvali
SLAC-PUB-7801

Motivation: Solve the hierarchy problem by removing it!



SM fields confined to 3-brane

Gravity becomes strong in the bulk

$$\text{Gauss' Law: } M_{\text{Pl}}^2 = V_\delta M_D^{2+\delta} \quad ; \quad V_\delta \sim R_c^\delta$$

M_D = Fundamental scale in the bulk
 $\simeq \text{TeV}$

$\delta = 1$ $R_c \sim 10^{-11} \text{ m}$ Excluded!

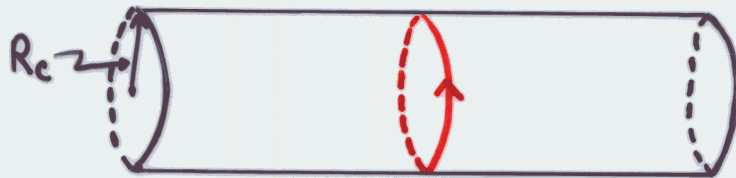
2 0.4 mm $m_c = 1/R_c \sim 5 \times 10^{-4} \text{ eV}$

4 10^{-5} mm 20 KeV

6 30 fm 7 MeV

Compactification: Bulk Fields

Bulk fields expand into Kaluza-Klein towers



6-d kinetic motion
is quantized!

$$p_s^2 = \frac{\vec{n} \cdot \vec{n}}{R_c^2}$$

mode numbers $\vec{n} = (n_1, n_2, \dots, n_s)$

label KK excitation state

Appears as tower of massive particles in 4-d

$$\Phi(x_m, y_i) = \sum_{\vec{n}=0}^{\infty} \phi^{(\vec{n})}(x_m) e^{i\vec{n} \cdot \vec{y}/R_c} \cdot \frac{1}{\sqrt{V_s}}$$

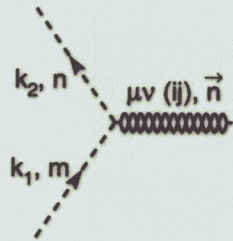
for periodic $y_i \rightarrow y_i + 2\pi R_c$ Flat space

$$\text{with mass } m_{\vec{n}}^2 = \frac{\vec{n} \cdot \vec{n}}{R_c^2}$$

KK tower of evenly spaced states
each with identical spin + quantum numbers

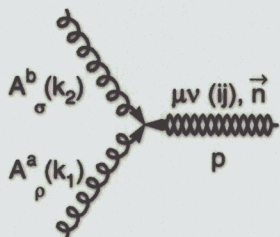
Feynman Rules - Graviton KK tower

Massless O-mode + KK states have identical coupling to matter

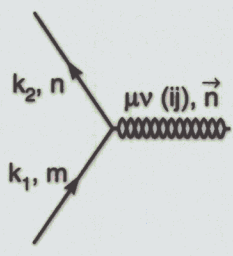


$$\begin{aligned}\tilde{h}_{\mu\nu}^{\vec{n}} \Phi\Phi &: -i\kappa/2 \delta_{mn} (m_\Phi^2 \eta_{\mu\nu} + C_{\mu\nu,\rho\sigma} k_1^\rho k_2^\sigma) \\ \tilde{\phi}_{ij}^{\vec{n}} \Phi\Phi &: i\omega\kappa \delta_{ij} \delta_{mn} (k_1 \cdot k_2 - 2m_\Phi^2)\end{aligned}$$

$$\kappa \sim \frac{1}{M_{Pl}}$$



$$\begin{aligned}\tilde{h}_{\mu\nu}^{\vec{n}} AA &: -i\kappa/2 \delta^{ab} ((m_A^2 + k_1 \cdot k_2) C_{\mu\nu,\rho\sigma} + D_{\mu\nu,\rho\sigma} (k_1, k_2) \\ &\quad + \xi^{-1} E_{\mu\nu,\rho\sigma} (k_1, k_2)) \\ \tilde{\phi}_{ij}^{\vec{n}} AA &: i\omega\kappa \delta_{ij} \delta^{ab} (\eta_{\rho\sigma} m_A^2 + \xi^{-1} (k_{1\rho} p_\sigma + k_{2\rho} p_\sigma))\end{aligned}$$



$$\begin{aligned}\tilde{h}_{\mu\nu}^{\vec{n}} \psi\psi &: -i\kappa/8 \delta_{mn} (\gamma_\mu (k_{1v} + k_{2v}) + \gamma_v (k_{1\mu} + k_{2\mu}) \\ &\quad - 2\eta_{\mu\nu} (k_1 + k_2 - 2m_\psi)) \\ \tilde{\phi}_{ij}^{\vec{n}} \psi\psi &: i\omega\kappa \delta_{ij} \delta_{mn} (3/4 k_1 + 3/4 k_2 - 2m_\psi)\end{aligned}$$

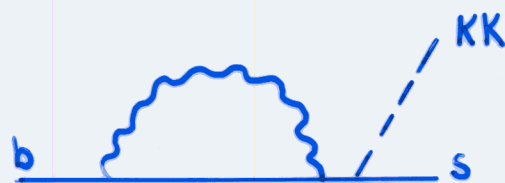
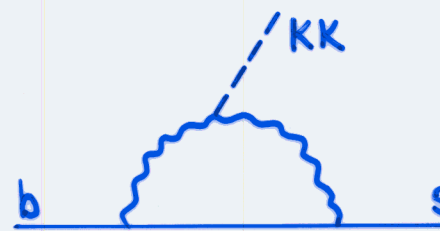
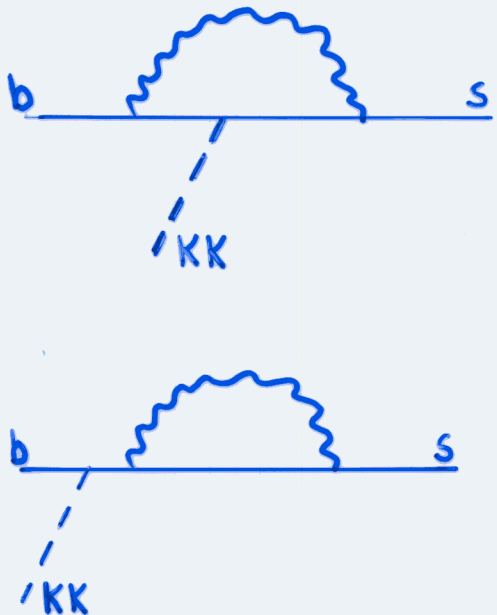
Figure 4: Three-point vertex Feynman rules. The KK states are plot in double-sinusoidal curves. The symbols $C_{\mu\nu,\rho\sigma}$, $D_{\mu\nu,\rho\sigma}(k_1, k_2)$ and $E_{\mu\nu,\rho\sigma}(k_1, k_2)$ are defined in Eqs. (A.10), (A.11) and (A.12) respectively. m_Φ , m_A and m_ψ are masses of the scalar, vector and fermion. $\omega = \sqrt{\frac{2}{3(n+2)}}$, $\kappa = \sqrt{16\pi G_N}$ and ξ is the gauge-fixing parameter.

Han, Lykken, Zhang
Giudice, Rattazzi, Wells

$B \rightarrow X_s + \text{Missing : Graviton Emission}$

Mahajan
hep-ph/0211255

Dilaton KK emission:



Induces new operators:

$$O_{\text{Dilaton}} \sim \bar{s}(1 \pm \gamma_5)b \Phi$$

$$O_{\text{Graviton}} \sim \bar{s} \gamma_\mu p_\nu(b)(1 - \gamma_5)b h^{\mu\nu}$$

$$\mathcal{M}(b \rightarrow s \Phi) = \frac{i G_F \omega_X}{16 \pi^2} \ln \frac{\Lambda^2}{m_W^2} \gtrsim_t m_t^2 \frac{m_b}{3}$$

$\xleftarrow{\frac{1}{m_{Pl}}}$

$$\left[18 \frac{m_s^2}{m_b^2 - m_s^2} - 1 \right] \bar{s}(1 + \gamma_5)b$$

Perform sum over KK tower:

$$\Gamma \sim \frac{1}{m_{Pl}^2} (m_b R_c)^\delta \rightarrow \frac{1}{m_D^2} \left(\frac{m_b}{m_0} \right)^\delta$$

$B(B \rightarrow X_s \bar{\Phi})$	δ	$m_0 (\text{TeV})$
1.28×10^{-3}	2	1
2.25×10^{-6}	3	1
4.93×10^{-9}	4	1
5.50×10^{-6}	2	5
1.93×10^{-9}	3	5
8.45×10^{-13}	4	5

$$B(B \rightarrow X_s \nu \bar{\nu})_{\text{SM}} \sim 5 \times 10^{-5}$$

$$B(B \rightarrow X_s \nu \bar{\nu})_{\text{exp}} < 6.2 \times 10^{-4} \text{ @ 90% CL}$$

LEP Bound: Graviton emission

$$\delta=2, m_0 > 1.28 \text{ TeV}$$

$\Rightarrow B \rightarrow X_s \bar{\Phi}$ is comparable to collider searches!

Flavor Physics in Extra Dimensions - Basic Ingredients

String/M-Theory $\Rightarrow n = 6, 7$

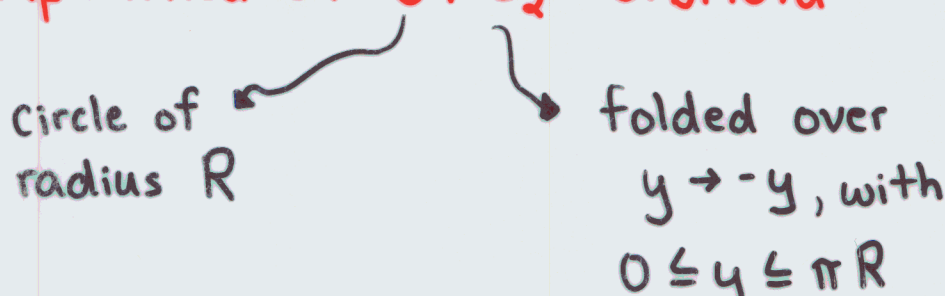
Let $R^n = R_1^p R_2^{n-p}$ with $R_1 \sim \text{large}$
 $R_2 \sim \text{small} \sim 1/\text{Tev} \sim 1/m_*$

$$\begin{aligned} \Rightarrow M_{Pl}^2 &= R_1^p m_*^{p-n} m_*^{n+2} \\ &= R_1^p m_*^{p+2} \quad \text{with } 2 \leq p \leq 6 \end{aligned}$$

SM fields can propagate in small R_2^{n-p} dimensions

Consider 5DSM: 1 extra $1/\text{Tev}$ dimension (Antoniadis)
flat, factorizable geometry

(x^μ, y) with y compactified on S^1/Z_2 orbifold

circle of radius R 
folded over $y \rightarrow -y$, with $0 \leq y \leq \pi R$

3D branes located at orbifold fixed points

Examine 5-D Action

$$S_5 = \int d^4x \int dy [S_{\text{SMGF}} + S_{\text{Higgs}} + S_{\text{fermions}}]$$

integrate to get 4-D effective theory

KK excitations of gauge fields

$$\gamma_n, z_n, w_n, g_n$$

- degenerate (up to mixing)

$$m_n = n/R$$

- Equally spaced states

$$\alpha_{(n)} = 2 \alpha_{(0)}$$

Contribute to EW precision observables

$$\Rightarrow m_c \sim 1/R \gtrsim 2-5 \text{ TeV}$$

Rizzo, Wells

Can lead to drastic lowering of GUT scale

via \sim power-like running of couplings

Dienes, Dudas,
Ghergetta

Universal Extra Dimensions

Appelquist et al

Full SM is in the bulk!

and expands into KK towers...

Branes need not be present \Rightarrow translational invariance preserved in full spacetime.

Conservation of KK parity $(-1)^n$

KK states occur in pairs in production + in loops

Drastic reduction in precision EW constraints:

$$R_c' \gtrsim 400 - 500 \text{ GeV}$$

KK Contributions to $B \rightarrow X_s \gamma$

Agashe, Deshpande,
Wu

W-top KK loops:

$$C_7(m_w) \sim \sum_n \frac{m_t^2 m_w^2}{(n/R_c)^4}$$

Goldstone Boson-top KK loops:

$$C_7(m_w) \sim \sum_n \left[1 + \frac{m_t^2}{(n/R)^2} \right] \left[A \left(\frac{m_t^2}{(n/R)^2} \right) - \frac{1}{6} B \left(\frac{m_t^2}{(n/R)^2} \right) \right]$$

loop integrals

No new operators are induced

Comparison with data:

$$R_c^{-1} \gtrsim 280 \text{ GeV}$$

Comparable to precision EW constraints!

Two Higgs Doublets in the bulk:

Constraints
from
 $B \rightarrow X_s \gamma$

Agashe, Deshpande,
Wu

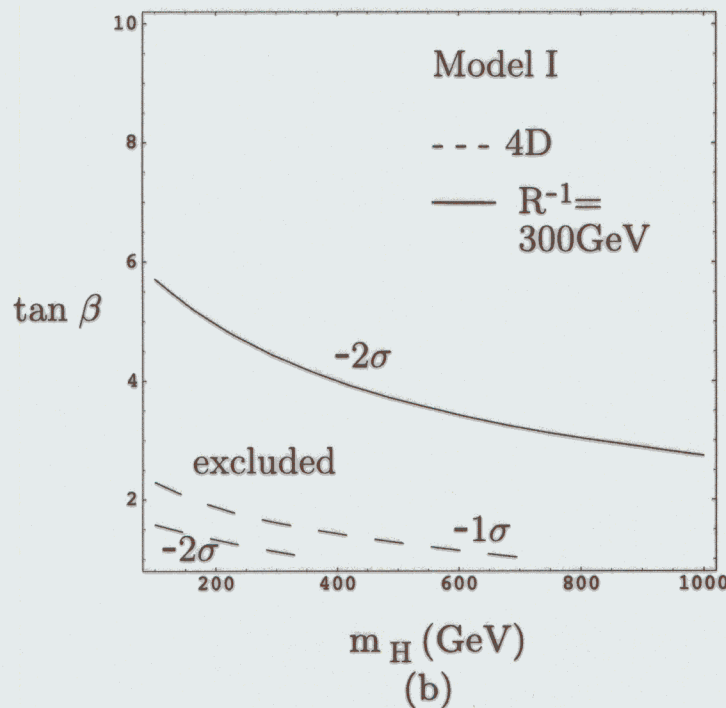
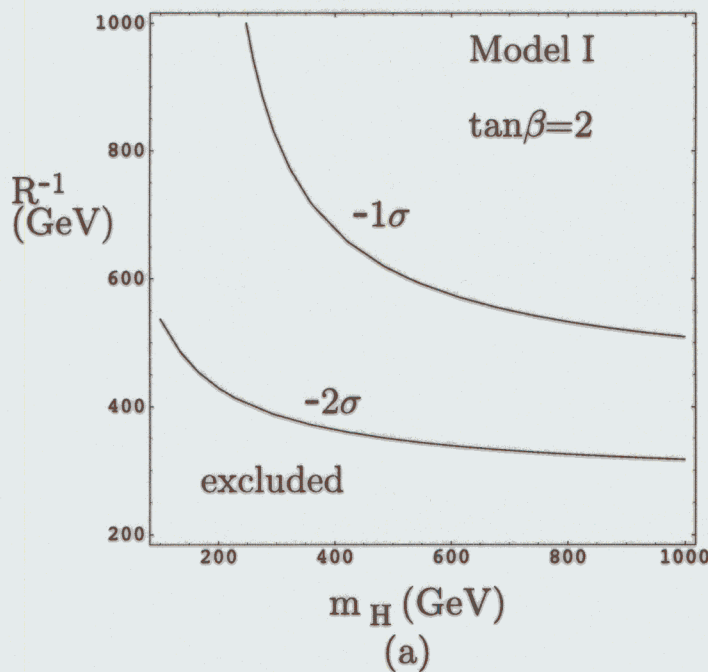


Figure 2: The deviation of the rate of $b \rightarrow s\gamma$ from the SM prediction in model I as a function of size of one extra dimension (R^{-1}) and charged Higgs mass (m_H) for $\tan\beta = 2$ (figure (a)) and as a function of $\tan\beta$ and m_H for $R^{-1} = 300$ GeV (figure (b)). In figure (b), the dashed lines are the result in 4D. The 1σ deviation corresponds to 18%.

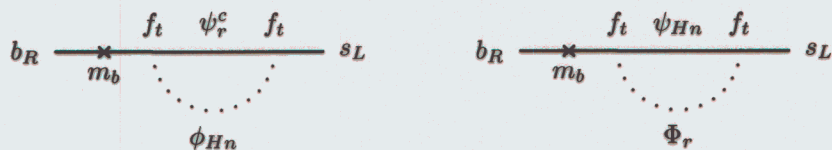
Supersymmetric Extra Dimensions

Barbieri + Hall

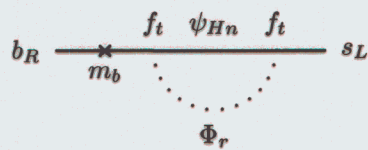
5D SUSY compactified on $S^1/Z_2 \times Z'_2$

Double orbifolding breaks EW symmetry !!

$B \rightarrow X_s \gamma$:



(a)

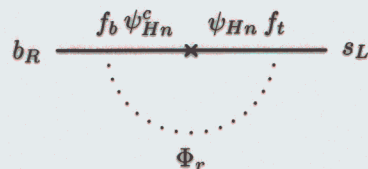


(b)

+ attached γ

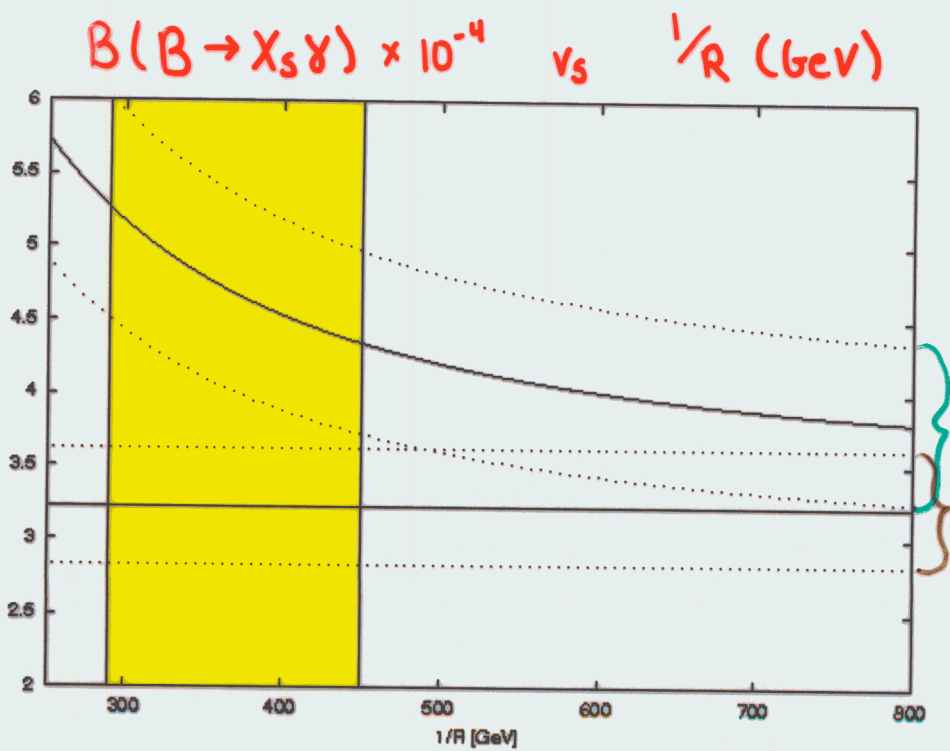


(c)



(d)

Barbieri, Cacciapaglia,
Romito



Shaded region:
theoretically favored
to obtain light
Higgs

prediction

Exp

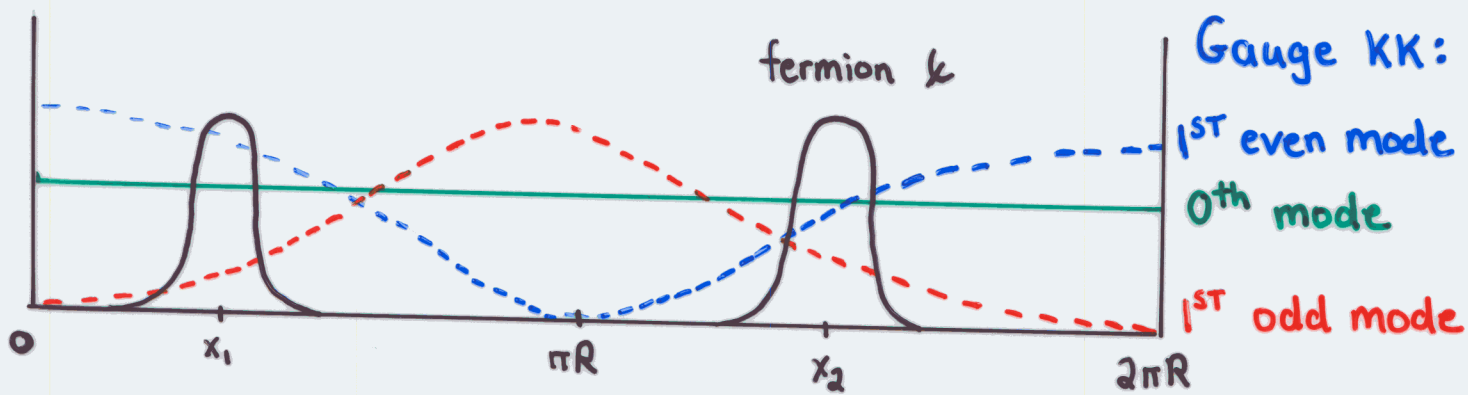
Fat Branes - SM lives in a Thick brane

Antoniadis

- One Scenario:
- SM gauge fields live throughout
 - SM fermions localized at specific points within brane

- Motivations:
- suppress proton decay
 - achieve gauge coupling unification
 - generate fermion mass hierarchy

Precision EW Data Constrains $R_c^{-1} \gtrsim 2\text{-}5 \text{ TeV}$



$$x^n(\theta) = \begin{cases} \frac{1}{\sqrt{2\pi}}, & n=0 \\ \frac{\cos n\theta}{\sqrt{\pi}}, & n \neq 0 \end{cases}$$

Arkani-Hamed, Schmaltz

Fermion mixing induces FC KK interactions

Wavefunction Overlap:

$$x_i = \int d\theta \bar{f}_i(\theta) f_i(\theta) X^n(\theta) ; \quad f(\theta) = \begin{matrix} \text{narrow} \\ \text{Gaussian} \end{matrix}$$

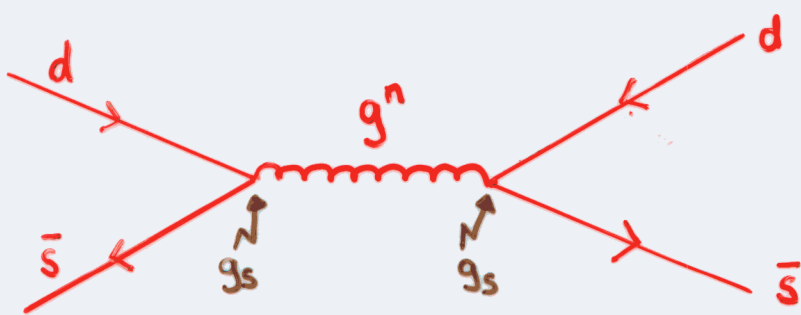
$$\simeq \cos n\theta_i \quad \text{in weak basis}$$

In mass eigenstate basis:

$$X_{ij} = (U^+)_i k x_k \delta_{ik} U_{aj}$$

leads to flavor changing couplings!

K- \bar{K} mixing:



Tree-level FCNC with strong couplings!

$$\frac{1}{R_c} \gtrsim 400 \text{ TeV} \left[\frac{\sum_n X_{sd}/n}{0.3} \right]$$

Delgado, Pomarol,
Quirós
hep-ph/9911252

Poses a threat to the model! Further study needed...

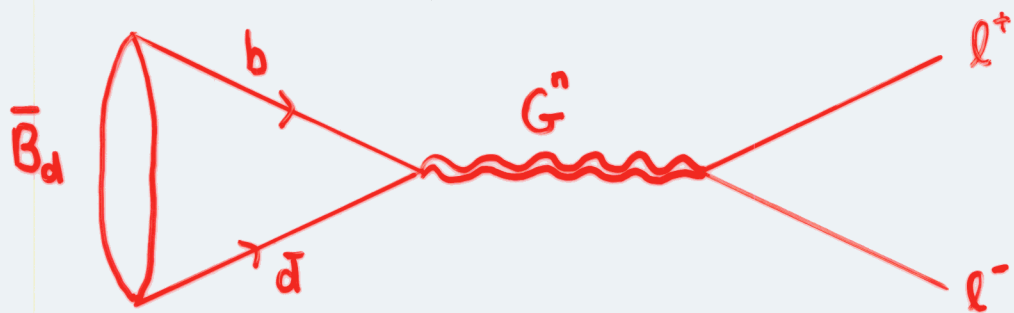
$\text{AdS}_5 \times S^5/\mathbb{Z}_2$

Davoudiasl, JLH, Rizzo
hep-ph/0211377

Attempt to embed Randall-Sundrum model of localized gravity within string theory

TeV scale KK gravitons with TeV^{-1} couplings

Fermion mixing induces FC KK graviton interactions!



$$\Gamma(B_d \rightarrow l^+ l^-) \sim \frac{f_B^2 m_B^5 m_\ell^2}{\Lambda_\pi^4 m_{lo}^4} \left| \sum_{n,m} \frac{x_{lo}^2 [x_L^{gb} - x_R^{gb}] [x_L^l - x_R^l]}{\overline{x_{nm}^2}} \right|^2$$

\Rightarrow is highly suppressed!

Further study needed...

Model Dependent New Physics Summary

Table 13–6. Model dependent effects of new physics in various processes.

Model	$B_d^0 - \bar{B}_d^0$ Mixing	CP Violation			$D^0 - \bar{D}^0$ Mixing
MSSM	$\mathcal{O}(20\%)$ SM Same Phase	No Effect		$B \rightarrow X_s \gamma$ – yes $B \rightarrow X_s l^+ l^-$ – no	No Effect
SUSY – Alignment	$\mathcal{O}(20\%)$ SM New Phases	$\mathcal{O}(1)$		Small Effect	Big Effect
SUSY – Approx. Universality	$\mathcal{O}(20\%)$ SM New Phases	$\mathcal{O}(1)$	No Effect		No Effect
R -Parity Violation	Can Do	Everything	Except Make		Coffee
MHDM	\sim SM/New Phases	Suppressed	$B \rightarrow X_s \gamma, B \rightarrow X_s \tau \tau$		Big Effect
2HDM	\sim SM/Same Phase	Suppressed	$B \rightarrow X_s \gamma$		No Effect
Quark Singlets	Yes/New Phases	Yes	Saturates Limits	$Q = 2/3$	
Fourth Generation	\sim SM/New Phases	Yes	Saturates Limits		Big Effect
$LRM - V_L = V_R$ $- V_L \neq V_R$	No Effect Big/New Phases	No Effect Yes	$B \rightarrow X_s \gamma, B \rightarrow X_s l^+ l^-$ $B \rightarrow X_s \gamma, B \rightarrow X_s l^+ l^-$	No Effect No Effect	No Effect
DEWSB	Big/Same Phase	No Effect	$B \rightarrow X_s \ell \ell, B \rightarrow X - s \nu \bar{\nu}$		Big Effect

+ Extra Dimensions! + Little Higgs!